Age of stratospheric air in the ERA-Interim

M. Diallo, B. Legras, A. Chédin

Atmos. Chem. Phys., 12, 12133–12154, 2012
www.atmos-chem-phys.net/12/12133/2012/
doi:10.5194/acp-12-12133-2012

Atmospheric Chemistry and Physics

Age of stratospheric air in the ERA-Interim

M. Diallo[1], **B. Legras**[1], **and A. Chédin**[2]

[1]Laboratoire de Météorologie Dynamique, UMR8539, IPSL, UPMC/ENS/CNRS/Ecole Polytechnique, Paris, France
[2]Laboratoire de Météorologie Dynamique, UMR8539, IPSL, CNRS/Ecole Polytechnique/ENS/UPMC, Palaiseau, France

Correspondence to: M. Diallo (mdiallo@lmd.ens.fr)

Received: 14 June 2012 – Published in Atmos. Chem. Phys. Discuss.: 11 July 2012
Revised: 25 October 2012 – Accepted: 30 November 2012 – Published: 21 December 2012

Abstract. The Brewer-Dobson mean circulation and its variability are investigated in the ERA-Interim over the period 1989-2010 by using an off-line Lagrangian transport model driven by analysed winds and heating rates.

At low and mid-latitudes, the mean age of air in the lower stratosphere is in good agreement with ages derived from aircraft, high altitude balloon and satellite observations of long-lived tracers. At high latitude and in the upper stratosphere, we find, however that the ERA-Interim ages exhibit an old bias, typically of one to two years.

The age spectrum exhibits a long tail except in the low tropical stratosphere which is modulated by the annual cycle of the tropical upwelling. The distribution of ages and its variability is consistent with the existence of two separate branches, shallow and deep, of the Brewer-Dobson circulation. Both branches are modulated by the tropical upwelling and the shallow branch is also modulated by the subtropical barrier.

The variability of the mean age is analysed through a decomposition in terms of annual cycle, QBO, ENSO and trend. The annual modulation is the dominating signal in the lower stratosphere and is maximum at latitudes greater than 50° in both hemispheres with oldest ages at the end of the winter. The phase of the annual modulation is also reversed between below and above 25 km. The maximum amplitude of the QBO modulation is of about 0.5 yr and is mostly concentrated within the tropics between 25 and 35 km. It lags the QBO wind at 30 hPa by about 8 months. The ENSO signal is small and limited to the lower northen stratosphere.

The age trend over the 1989–2010 period, according to this ERA-Interim dataset, is significant and negative, of the order of -0.3 to $-0.5\,\mathrm{yr\,dec^{-1}}$, within the lower stratosphere in the Southern Hemisphere and south of 40° N in the Northern Hemisphere below 25 km. The age trend is positive (of the order of $0.3\,\mathrm{yr\,dec^{-1}}$) in the mid stratosphere but there is no region of consistent significance. This suggests that the shallow and deep Brewer-Dobson circulations may evolve in opposite directions.

Finally, we find that the long lasting influence of the Pinatubo eruption can be seen on the age of air from June 1991 until the end of 1993 and can bias the statistics encompassing this period.

1 Introduction

Over the last twenty years, the Brewer-Dobson circulation has been recognized as a major component of the climate system (Andrews et al., 1987; Holton et al., 1995; Salby and Callaghan, 2005, 2006) which affects radiative budget and atmospheric circulation.

Reanalysed winds from operational weather centres are used to drive Chemistry Transport Models (CTM). Therefore, they are required to properly represent the Brewer-Dobson circulation in order to account for the dependence of the distribution of chemical species in the stratosphere onto the transport properties. It is also important per se to assess the ability of the combined system of a numerical weather forecast model and the associated assimilation system to reproduce the observed behaviour of the stratospheric circulation.

A commonly used metric of the Brewer-Dobson circulation is the *age of air*, defined as the time spent by a particle in the stratosphere since its entry across the tropopause (Li and Waugh, 1999; Waugh and Hall, 2002). As each air parcel is a mixture of particles with different histories and ages, the age of the parcel is an average over these particles (Kida, 1983; Hall and Plumb, 1994). The age can be further

Published by Copernicus Publications on behalf of the European Geosciences Union.

averaged over time and space to define a *mean age* over this ensemble or can be described as a distribution denoted as the *age spectrum* (Waugh and Hall, 2002). A main advantage of the age of air is that it can be estimated from observations of long-lived species (Andrews et al., 2001b; Waugh and Hall, 2002; Stiller et al., 2008; Garcia et al., 2011). The age of air is also used as a mean to compare models (Eyring et al., 2006). The distribution of mean age in latitude and altitude is convenient to visualize the Brewer-Dobson circulation, its strength and its variability (Li and Waugh, 1999; Waugh and Hall, 2002; Austin and Li, 2006). The age spectrum further characterizes the variability and the distribution of transport paths and mixing in the stratosphere (Andrews et al., 1999; Schoeberl et al., 2003, 2005; Reithmeier et al., 2008; Li et al., 2012).

Another metric of the Brewer-Dobson circulation is based on the calculation of the residual vertical and meridional velocities (Andrews et al., 1987) which are a representation of the mean zonally averaged mass transport in the stratosphere. This *residual circulation* is used to calculate transit times from the tropopause crossing (see, e.g. Birner and Bonisch, 2011). Transit times, however, are generally not identical to the age of air as this latter is also influenced by fast stirring and mixing induced by horizontal quasi-isentropic motion in the stratosphere (Waugh and Hall, 2002; Birner and Bonisch, 2011).

The Brewer-Dobson circulation undergoes an annual cycle and changes from year to year. A major mode of variability is the quasi-biennial oscillation (QBO) (Baldwin et al., 2001) which triggers a modulation of vertical transport in the stratosphere by affecting temperature and thus heating rates (Niwano et al., 2003; Punge et al., 2009). An other important factor are volcanic eruptions: in 1991, the Pinatubo has injected massive amount of dust in the stratosphere which have affected its circulation for several years (Thompson and Solomon, 2009). ENSO (Shu et al., 2011) and solar variations are two other sources of Brewer-Dobson variability.

A major source of concern is the existence of a trend in the Brewer-Dobson circulation. Changes in wave propagation and dissipation, as well as possible increases in tropospheric wave activity, are thought to be the primary driver of a strengthened Brewer-Dobson circulation obtained in many models (Butchart and Scaife, 2001; Sigmond et al., 2004; Butchart et al., 2006; Li et al., 2008; Garcia and Randel, 2008). Thompson and Solomon (2005) have observed a cooling of the tropical stratosphere in radiosonde records over the last decades, which is consistent with increased upwelling in the tropical stratosphere.

The analysis of tracer data, however, does not provide evidence for such trend. Engel et al. (2009) and Stiller et al. (2012) even suggest than the age of air might be increasing in some parts of the stratosphere. A possible reason for this discrepancy is that short term trends over one decade are not representative of the trend over one century (Waugh, 2009). Another possibility, however, is that the models or the diagnostics do not fully account for the stratospheric processes. Ray et al. (2010) analysed the observed trends in mean age and ozone, assuming a simple tropical pipe model, and concluded that “the best quantitative agreement with the observed mean age and ozone trends over the past three decades is found assuming a small strengthening of the mean circulation in the lower stratosphere, a moderate weakening of the mean circulation in the middle and upper stratosphere, and a moderate increase in the horizontal mixing into the tropics”. Similarly, Bonisch et al. (2011) found an increase of the Brewer-Dobson circulation in the lower stratosphere but no change at upper levels. In another recent study, Monge-Sanz et al. (2012) found a small old trend of the ages in the same ERA-Interim data used in the present study.

In this study, we present the age of stratospheric air over the period 1989–2010 from Langrangian transport calculations based on most recent reanalysed winds and heating rates from the ERA-Interim reanalysis of the European Centre for Medium Range Weather Forecast (ECMWF). The age of stratospheric air is investigated using backward deterministic trajectories which are integrated over 10 yr in time to evaluate the residence time in the stratosphere. We describe the method and data used in this study in Sect. 2. The mean climatology of the age of air is discussed and compared with observations in Sect. 3. The age variability, the impact of annual cycle and QBO, and the age trend are discussed in Sect. 4. Section 5 provides further discussions and conclusions.

2 Method and data

2.1 Backward trajectories

Backward deterministic trajectories are calculated using the Lagrangian model TRACZILLA (Legras et al., 2005) which is a modified version of FLEXPART (Stohl et al., 2005). TRACZILLA uses analysed winds to move particles in the horizontal direction and performs direct interpolations from data on hybrid levels. In the vertical direction, it uses either pressure coordinate and Lagrangian pressure tendencies, or potential temperature coordinate and heating rates. In the first case, we denote the trajectories as *kinematic* and in the second case as *diabatic* following a convention established by Eluszkiewicz et al. (2000). At each vertical level, particles are initialised over a longitude-latitude grid with 2° resolution in latitude and an almost uniform spacing in longitude of $2°/\cos(\phi)$, where ϕ is the latitude, generating 10 255 particles on each level. For convenience the vertical levels of the initial grid are chosen to be the hybrid levels of the ECMWF model. In order to encompass the whole stratosphere at any latitude, the 30 levels from about 400 hPa (varying according to the surface pressure) to 2 hPa are selected. Trajectories starting below the tropopause are immediately stopped and therefore do not induce any computational cost. Particles starting in the stratosphere are integrated backward in time until they cross the tropopause (see Sect. 2.3). Ensembles of particles have been launched at the end of every month over the period 1989–2010 and they are integrated backward for 10 yr.

2.2 Data

The wind data and heating rates used in this study have been produced by the ERA-Interim reanalysis of ECMWF (Dee et al., 2011). This reanalysis uses a 12 h 4D-Var assimilation cycle with a T255 partially desaliased horizontal truncature in spherical harmonics and 60 hybrid levels in the vertical from the surface to 0.1 hPa or 66 km. The model has, on the average, 8 levels between 300 and 100 hPa which encompass the extra-tropical lower stratosphere and the tropical tropopause layer and 25 levels above 100 hPa. Wind fields are extracted from the analysis available at 6 h interval (00:00 UT, 06:00 UT, 12:00 UT and 18:00 UT). They are completed by wind fields from 3 h and 9 h forecasts at 03:00 UT, 09:00 UT, 15:00 UT and 21:00 UT. Heating rates are obtained as temperature tendencies at 3 h intervals from the twice-daily assimilation cycles starting at 00:00 UT and 12:00 UT. Hence they are available at 01:30 UT, 04:30 UT, 07:30 UT, 10:30 UT, 13:30 UT, 16:30 UT, 19:30 UT and 22:30 UT.

Several studies have shown that winds from analysis or reanalysis are noisy and induce unrealistic diffusive transport and too fast apparent Brewer-Dobson circulation in the stratosphere (Schoeberl et al., 2003; Meijer et al., 2004; Scheele et al., 2005). This effect is mostly noticed in the vertical direction where velocities are naturally very small. There are two main reasons for this behaviour. The first is the gravity wave noise induced by the assimilation system. Such noise is transient and dampened during subsequent evolution so that medium-range forecasts exhibit less diffusion than the analysis (Stohl et al., 2005; Legras et al., 2005). This effect is pronounced in assimilation systems using 3D-Var assimilation, like in the ERA-40, and is significantly reduced with 4D-Var assimilation, like in the ERA-Interim. The second reason lies in the fact that archived analysis used for off-line transport studies are instantaneous winds typically sampled at 6 h interval. As a result, fast perturbations with time-scale smaller than 6 h are under-sampled. In the limit of very fast uncorrelated perturbations, a sampling with interval τ induces a spurious diffusion which is proportional to τ. Other reasons might be found in the parameterisations of gravity-wave drag, the representation of convection and the radiative calculations.

The undersampling effect can be reduced by using higher sampling rates at 3 h resolution (Stohl et al., 2005; Legras et al., 2005) or averaging the wind field (Schoeberl et al., 2003; Schoeberl and Dessler, 2011) as both tend to reduce the noise. There are indications (Pisso and Legras, 2008) that increasing the sampling rate to 1 h does not improve the noise in the stratosphere with current generation of reanalysis.

There are several reasons for which the vertical motion, as represented by heating rates in isentropic coordinates, is expected to be less noisy than that represented by vertical velocities in pressure coordinates. Using isentropic coordinates in the vertical separates the fast isentropic motion from slower vertical cross-isentropic motion in the stratosphere and avoids spurious numerical transport effects when particles move with respect to oscillating isobaric surfaces. Another reason is that the heating rates are usually archived as accumulations over finite periods and not as instantaneous values like the velocities. Consequently, the heating rates integrate the noisy fluctuations and are much smoother in time and space than the kinematic velocities.

Data from the ERA-Interim have been used from 1979 to 2010. Since backward trajectory calculations are performed over a duration of 10 yr, the age of air has been estimated monthly over a 22-yr period between 1989 and 2010. For the sake of comparison with the ERA-40 reanalysis and the calculations of Monge-Sanz et al. (2007), some integrations with a perpetual 2000 year have also been performed.

2.3 Metric of Brewer-Dobson circulation

The residence time of a particle in the stratosphere since it has crossed the tropopause, is defined as the *age of air* (Waugh and Hall, 2002) and is a common metric of the Brewer-Dobson circulation. As each air parcel results from the mixing of a large number of particles with different trajectories within the stratosphere, the age is actually distributed over a range of values for all the particles contributing to a given parcel. This distribution is denoted as the *age spectrum* which can be mathematically defined (Kida, 1983; Hall and Plumb, 1994; Waugh and Hall, 2002) as generated by a Green function describing the probability that a particle located at the tropopause at time $t-\tau$ is found within the considered parcel at time t. The first moment of the distribution of τ is the *mean age*.

The age of air can be retrieved from trace chemical species, such as sulfur hexafluoride SF_6 and carbon dioxide CO_2 which are well-mixed in the troposphere with a known trend and are nearly passive tracers in the stratosphere (SF_6 is only oxidized in the mesosphere and CO_2 has limited sources through the oxydation of CH_4) (Andrews et al., 2001a; Waugh and Hall, 2002; Stiller et al., 2008; Garcia et al., 2011). Such quantities have been measured from aircraft and balloons for several decades (Andrews et al., 2001a) and more recently from satellites (Stiller et al., 2008, 2012; Foucher et al., 2011). These data are used in this study in order to compare modelized ages to observations. The comparison to more recent observations of CO_2 stratospheric profiles from ACE-FTS (Foucher et al., 2009, 2011) will be presented in further studies. It is in principle possible to derive the full age spectrum if a large density of observations of tracers with

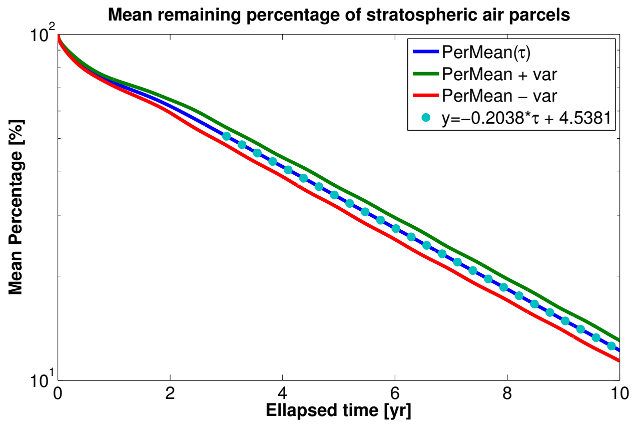

Fig. 1. Mean percentage of remaining air parcels in the stratosphere as a function of elapsed time τ (age). (Blue): mean over the 264 months of the 22-yr range. Basis 100 at time 0. (Green and red): mean $\pm$ one standard deviation. (Dotted): fit of the mean by the exponential decay law $93.48\exp(-0.2038\tau)$ where τ is in yr.

different life times is available (Andrews et al., 1999, 2001b; Schoeberl et al., 2005; Bonisch et al., 2009), but in practice only the mean age can be retrieved without ad hoc assumptions on the age distribution.

In our backward calculations, the age along a given backward trajectory is obtained as the time of first crossing of the tropopause, defined as the lower envelope of the surfaces $\theta = 380\,\mathrm{K}$ and $|P| = 2\times10^{-6}\,\mathrm{K\,kg^{-1}\,m^2\,s^{-1}}$ where P is the Ertel potential vorticity. The mean age for a given box in latitude and altitude (typically $2^\circ\times$ model level spacing) and for a given month is calculated as the average in longitude over all particles falling within this box. Owing to the quasi-uniform spread of the discrete trajectories at the initialisation stage, the average is made over 180 particles at the equator and over 67 particles at 68° N or S. Latitudes closer to the pole are grouped into enlarged latitude bins (69°–73°, 73°–77°, 77°–81°, 81°–90°) to avoid large fluctuations due to the reduced number of particles. Further averaging over time is performed to improve statistics and to reduce noise. These averaging procedures are a simple way to account for mixing in the stratosphere and gather within each box a distribution of particles with different histories.

As observed by Scheele et al. (2005), the number of backward trajectories launched at a given date and remaining within the stratosphere after some delay τ decreases exponentially with τ. Figure 1 shows that this law is indeed very well satisfied for $\tau > 3\,\mathrm{yr}$ with an exponential decrement $b = 0.2038\,\mathrm{yr}^{-1}$ for the mean decay and that the standard deviation from the mean (when each month is considered separately) decays at the same rate. After 10 yr of backward motion, 88 % of the particles launched within the stratosphere have met the tropopause. We follow Scheele et al. (2005) in using this property to correct the estimated ages for the truncature of trajectory lengths at 10 yr. If we define $F(\tau)$ as the probability density of the age τ, the mean age is

$$\bar{\tau} = \int_0^\infty \tau F(\tau)d\tau. \tag{1}$$

The truncated version of this integral, up to $t_f = 10\,\mathrm{yr}$, can be calculated explicitly from the trajectory calculations. Assuming that $F(\tau) = F(t_f)\exp(-b(\tau - t_f))$ for $t > t_f$, the mean age can be estimated as

$$\bar{\tau} = \int_0^{t_f} \tau F(\tau)d\tau + F(t_f)\left(t_f + \frac{1}{b}\right). \tag{2}$$

In practice, the calculation is discretized in the following way. For a total of N particles, those with ages under t_f, which have crossed the tropopause during backward integration before t_f, are distributed in K ages bins between 0 and t_f with n_i particles in the bin i centered on time t_i. If M_f particles remain within the stratosphere at time t_f, the corrected mean over this ensemble is

$$\bar{\tau} = \frac{1}{N}\sum_{i=1}^{K} n_i t_i + \frac{M_f}{N}\frac{b\,t_f + 1}{b^2}. \tag{3}$$

The decrement coefficient b, shown in Fig. 1 as a time average, has been calculated over the whole stratosphere for each month. It varies by $\pm0.02\,\mathrm{yr}^{-1}$ over time. It has also been calculated as a 22-yr mean for each latitude and altitude box. The resulting correction to the mean age varies from zero to almost two years at high altitude and latitude. The impact of choosing one definition of the decrement or the other does not change the estimated age by more than 3 %. Hence, the correction which is not negligible per se is quite insensitive to the arbitrary details of the calculations.

Notice, however, that the mean value of b differs from our value by almost a factor 2 in Li et al. (2012) who found $b \approx 0.36$ using the GEOSCCM model. The comparison with this calculation is further discussed below.

3 Mean climatology of the age of air

3.1 Global distribution of the mean age

The mean diabatic age of air, obtained with diabatic trajectories, is calculated as a function of latitude and altitude after averaging over the 22-yr dataset between 1989 and 2010. The left panel of Fig. 2 shows that mean age contours follow the tropopause except in the tropics where they bend up as a result of the tropical upwelling. Gradients of the age of air are concentrated within the extra-tropical lowermost stratosphere with approximately 0.5 yr per km. In the mid extra-tropical stratosphere, the mean age of air varies between 6 and 7.5 yr, with maximum values near the poles, and is older

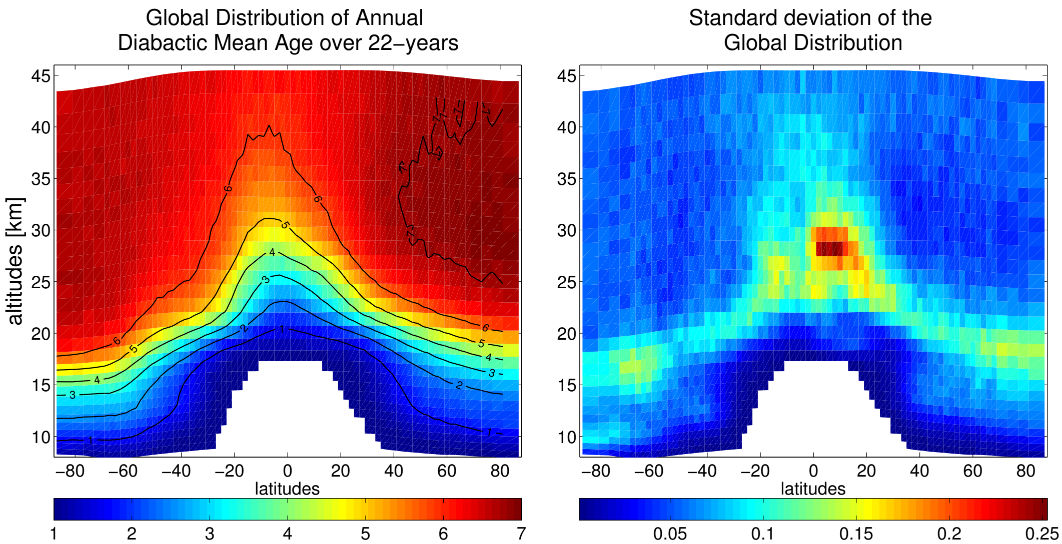

Fig. 2. (Left): distribution of mean age of stratospheric air (in yr) averaged over 22 yr (264 months, 1989-2010) as a function of latitude and altitude. (Right): estimated standard deviation of the mean age (in yr).

in the Northern Hemisphere above 25 km than in the Southern Hemisphere. The *tropical pipe* (Neu and Plumb, 1999), which confines the ascending branch of the Brewer-Dobson circulation above about 22 km, is revealed by young air moving upward in the tropics. This tropical pipe is slightly shifted from the equator with a maximum near 5° S. Its relative isolation is visualised by the horizontal age gradients on its northern and southern edges.

The right panel of Fig. 2 shows the standard deviation of the mean diabatic age calculated using the equivalent sampling size (see Appendix) that accounts for the time correlation of monthly ages. This standard deviation shows that the mean diabatic age is estimated with good accuracy within the framework of the ERA-Interim, with patterns that clearly offset the level of fluctuations. The variability of the mean age concentrates within a limited range of altitudes between 20 and 30 km and, as we shall see below, that the maximum of variance is correlated with the maximum of QBO wind modulation.

The difference between kinematic and diabatic ages, see Fig. 3, has been calculated over 35 months within the period 2006–2009. The pattern is quite unexpected with kinematic ages being older than diabatic ages in the lower stratosphere of the Southern Hemisphere and being younger between 22 and 40 km in the Northern Hemisphere. There is almost no difference in the southern mid-stratosphere and only a thin layer of older kinematic ages is visible in the northern lowermost stratosphere. It is usually found that kinematic velocities are noisier than diabatic heating rates resulting in a spurious vertical diffusion and a bias towards younger air (Schoeberl et al., 2003; Ploeger et al., 2010). However, the pattern of Fig. 3 cannot be explained by such a simple argument.

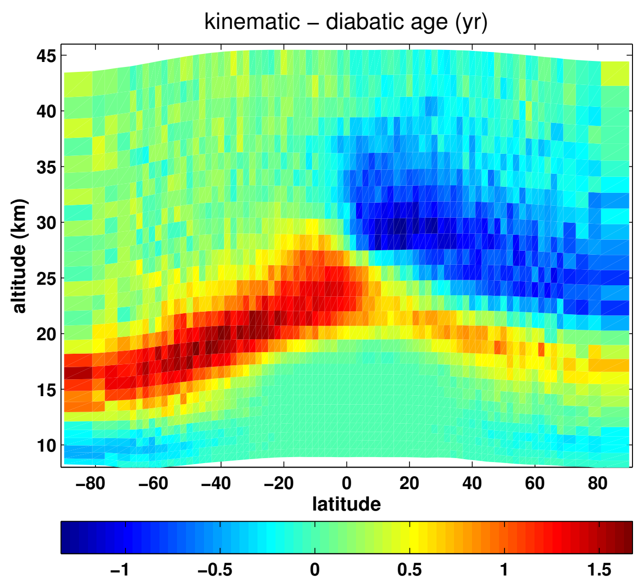

Fig. 3. Difference between mean kinematic age and mean diabatic age over 31 months in the period 2006-2009 (in yr).

In order to understand better the relation between air parcel origins and ages, Fig. 4 shows the distributions of maximum vertical excursion and of altitude of tropopause crossing. The distributions are shown separately for particles launched below 113 hPa in the extra-tropical lowermost stratosphere (lower row) and those launched at this level and above in the tropics and the extra-tropics (upper row), in the region of the stratosphere denoted as the *overworld* (Holton et al., 1995).

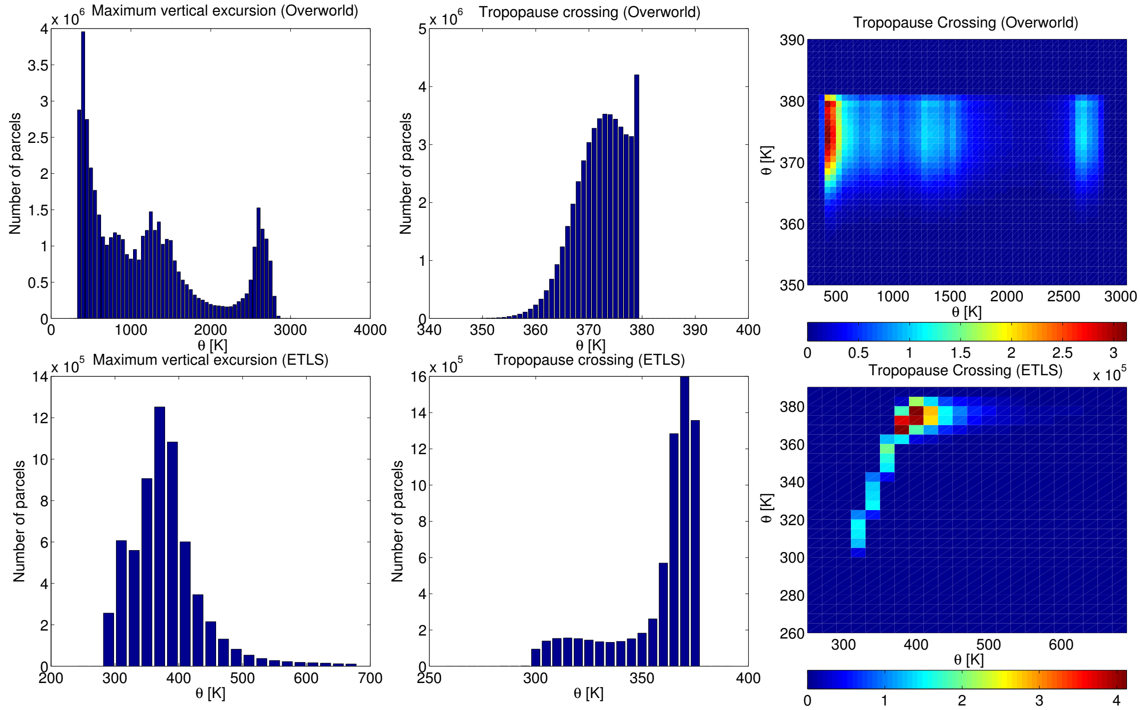

Fig. 4. Potential temperature distribution of maximum vertical excursion (left) and altitude of tropopause crossings (center) for the populations of particles launched in the extratropical lowermost stratosphere (bottom) and in the overworld (top). The vertical separation is made at the pressure level 113 hPa (level 26 of the ECMWF grid). The right panels show the joined histograms of vertical excursions and tropopause crossings. In the bottom panels the particles with vertical excursion larger than 700 K (6 % of the total) are not shown. The histograms are calculated over 22 yr and over the ensemble of particles which were located in the stratosphere at day 1 of the backward trajectory.

For overworld parcels, Fig. 4 shows that most of the entries to the stratosphere occur through the tropical tropopause between the isentropic levels 370–380 K. The histogram of maximum vertical excursion shows three maxima. The first one below 500 K corresponds to the fast branch of the Brewer-Dobson circulation which is bound to the lower stratosphere. The two other maxima are associated with the tropical pipe. The plume of air rising through the pipe is progressively stripped by detrainment to the mid-latitudes. Most particles reach a maximum value under 1500 K. Above this level, there is very little leakage from the tropical pipe between 1800 K and 2500 K and the third maximum near 2800 K is associated with particles reaching the top of the mesosphere in the model.

For particles initialised in the extra-tropical lowermost stratosphere, Fig. 4 shows that the majority of tropopause crossings still occur between 370 and 380 K in the tropics but a significant proportion of particles enter the stratosphere through the subtropical and extra-tropical tropopause at lower potential temperatures down to 300 K. The maximum vertical excursion is mainly contained within the 300–450 K range with a peak at 380 K. Only a small portion of the particles (about 6%, not shown), have maximum vertical excursion exceeding 700 K.

Hence, the low value and the strong gradient of the mean age above the extra-tropical tropopause are due to the combined effect of isentropic mixing of tropical and extra-tropical air across the subtropical tropopause and the fast shallow branch of the Brewer-Dobson circulation (Hoor et al., 2004; Bonisch et al., 2009). Although the deep branch of the Brewer-Dobson is important for the distribution of ages in the stratosphere and for stratospheric chemistry, it processes only a small portion of the air which circulates within the stratosphere and the air found within the lowermost extra-tropical stratosphere (except within the winter polar vortex) has been mainly processed through the shallow branch.

3.2 Comparison with observations and models

As a basis for comparison, we use the age of air obtained from in situ aircraft data prior to 1998 reported in Andrews et al. (2001a) and the ages derived from MIPAS retrieval of SF_6 in 2002–2004 (Stiller et al., 2008). Figure 5 shows that these two estimates overlap in the mid-latitudes but the SF_6 ages are older at high latitudes. This is consistent with the impact of photochemical dissociation of SF_6 in the mesosphere which contaminates the stratospheric air within the winter polar vortex (Waugh and Hall, 2002). However, according

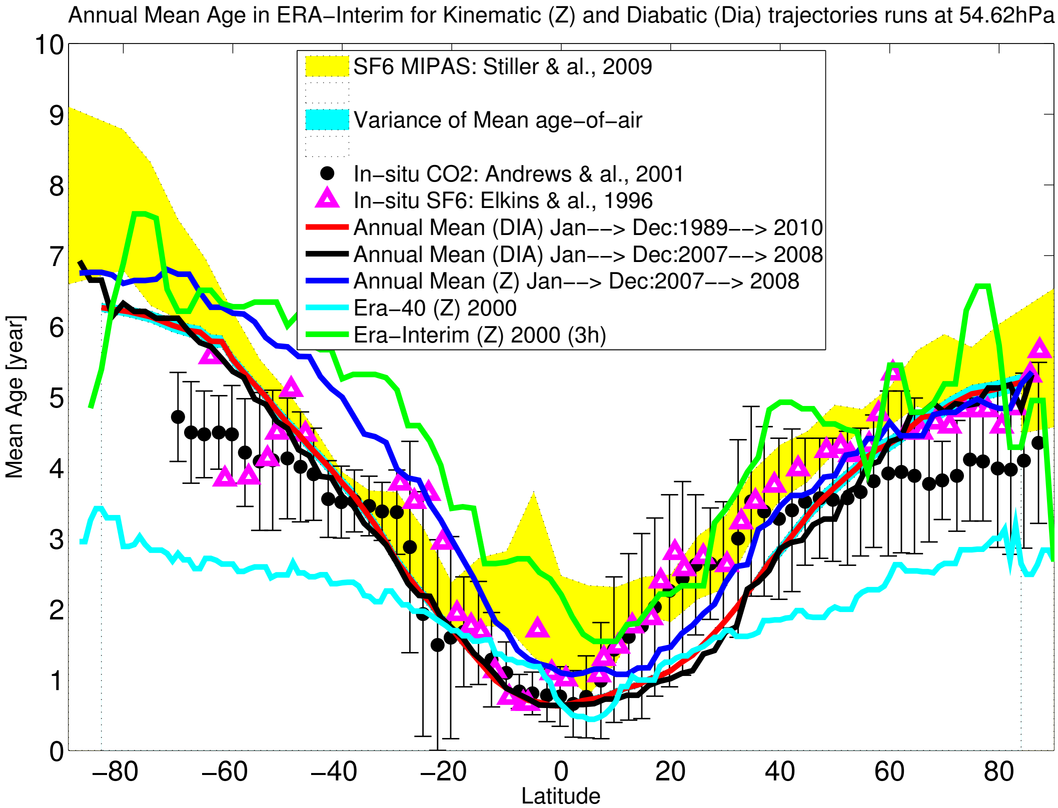

Fig. 5. Mean age of stratospheric air at 56 hPa (∼20 km) as a function of latitude, using ERA-Interim data unless specified. (Red): mean ages from diabatic trajectories averaged over 22 yr (1989–2010). (Blue): mean ages from kinematic trajectories averaged over 2 yr (2007–2008). (Black): mean ages from diabatic trajectories averaged over 2 yr (2007–2008). (Green): mean ages from kinematic trajectories and a perpetual run based on the year 2000 only. (Cyan): mean ages from kinematic trajectories and a perpetual run based on the year 2000 only with ERA-40 winds. (Yellow shaded area): envelope of mean ages from SF_6 MIPAS observations during November 2002–February 2003 and November 2003–February 2004 from Stiller et al. (2008). (Triangles): mean ages from airborne observations of SF_6 (Elkins et al., 1996; Waugh and Hall, 2002). (Dots and error bars): compilation of mean ages from airborne observations of CO_2 until 1998 by Andrews et al. (2001a). The error bar shows the statistical uncertainty of the mean age. The statistical uncertainty of the mean diabatic age is shown as ± one standard deviation (cyan shaded area) but this uncertainty is small enough to be hidden by the thickness of the red curve.

to Stiller et al. (2008), the systematic errors of age retrieval from SF_6 are such that ages are 0 to 0.5 yr too young in the lower stratosphere, even if they remain older than other observations.

Figure 5 shows that the ERA-Interim mean diabatic ages for the period 1989–2010 (red curve) are in good agreement with the aircraft observations except at high latitude. They are generally smaller than the MIPAS SF_6 ages by about 1 yr except in the southern mid-latitudes where the agreement between observations and simulation is the best. Consistently, the observations are less dispersed in this region. In the tropics the SF_6 MIPAS mean ages are about twice that of the ERA-Interim and in situ observations of SF_6 and CO_2. These comparisons should be appreciated with the reservation that observed and simulated ages are obtained over overlapping, albeit non identical, periods.

As already noticed the kinematic trajectories tend to produce significantly older ages in the Southern Hemisphere (black curve) at 20 km. These kinematic trajectories have been calculated for two years only, 2007 and 2008, but the discrepancy is meaningful because the diabatic ages averaged over the same years (blue curve) do not depart significantly from the 22-yr mean. This is contrasted with the kinematic trajectories calculated with winds from the ERA-40 reanalysis which tend to systematically produce younger ages (see Monge-Sanz et al., 2007, 2012, and cyan curve in Fig. 5). In the ERA-Interim, the statistics produced by kinematic and diabatic trajectories differ less than in the ERA-40 (Liu et al., 2010) but the difference is reversed. Schoeberl and Dessler (2011), using the MERRA reanalysis, found kinematic ages older than diabatic ages in the whole stratosphere and at the same time found an excessive vertical diffusion associated with the kinematic trajectories. Why kinematic trajectories produce longer residence time in the stratosphere or the type of pattern seen in Fig. 3 remains unclear. An excessive vertical diffusion should

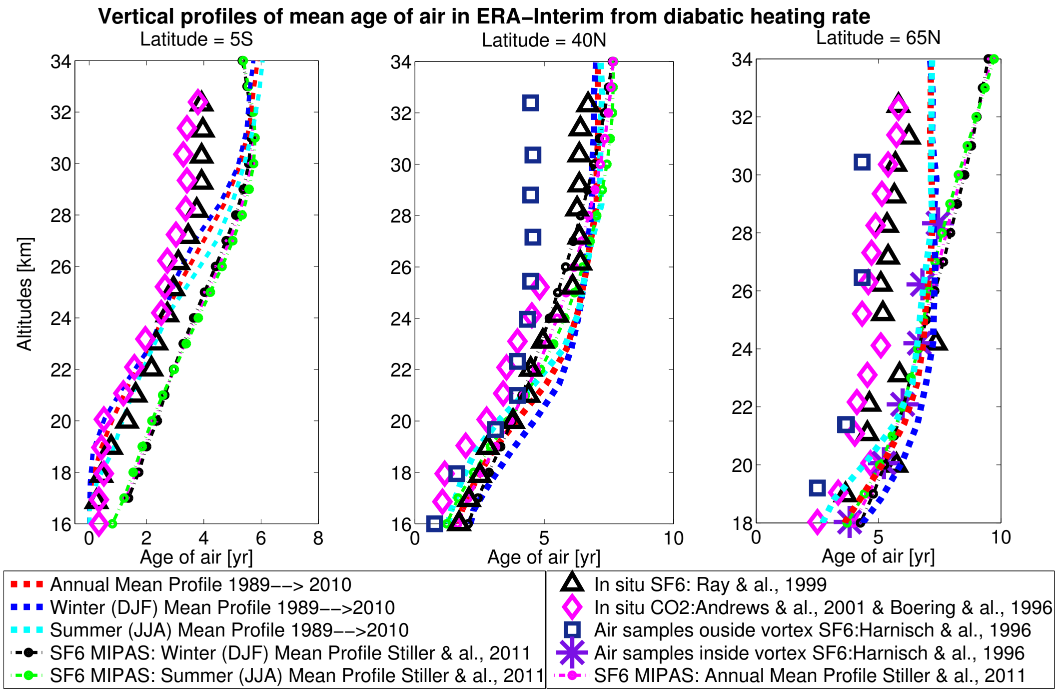

Fig. 6. (Dashed curves): vertical profiles of mean diabatic age (red: all year, blue: winter, cyan: summer). (Curves with circles): mean age profiles from SF_6 MIPAS (Stiller et al., 2012) (magenta: all year, black: winter, green: summer). (Symbols): in situ measurements of CO_2 (diamonds) (Boering et al., 1996; Andrews et al., 2001a), SF_6 (triangle) (Ray et al., 1999) and whole air samples of SF_6 (square outside vortex and asterisk inside vortex) (Harnisch et al., 1996).

produce younger ages, and reinforced exchanges between the tropics and the mid-latitudes should produce older ages in the tropics and younger ages in the mid-latitudes. None of these patterns is observed in Schoeberl and Dessler (2011) or in our study.

We stress that our calculations are all based on full historical records of velocity fields and heating rates over the length of the integration. In a number of previous studies, simulations using perpetual repetition of a given year have been used. This choice leads to considerable fluctuations of the age of air. For instance, the kinematic ages obtained for ERA-Interim based on a 2000 perpetual are significantly older than the 22-yr average (see Fig. 5) while its ERA-40 counterpart provides much too young ages. Large fluctuations, positive or negative, are also observed for diabatic trajectories calculated over perpetual years for 2000 and other years (not shown).

When compared with Chemistry-Climate-Model (CCM) estimates (Butchart et al., 2010), our ages based on Lagrangian trajectories are usually older, by about 1 yr in the tropics above 30 km and often 2 yr at mid and high latitudes. The horizontal gradient between the tropical pipe and the mid-latitudes is also stronger. However, a detailed comparison with a recent study of the age of air in the GEOSCCM (Li et al., 2012) reveals that the patterns of the age of air distributions, including its annual variations, are strikingly similar, even if the shift in the mean age just mentioned is still oberved. The comparison is performed in the Supplement where our results have been redrawn to produce figures that can be directly compared with those of Li et al. (2012). The differences in the mean ages may be partially due to differences in the numerical representation of tracer advection (Eluszkiewicz et al., 2000) as non diffusive Lagrangian calculations tend to produce older ages than other methods. Quite interestingly, it is shown in the supplement that discarding all particles travelling above $\theta = 1800\,K$ does not change the patterns of ages distribution but improves considerably the agreement with GEOSCCM ages. This suggests that trapping of particles near the lid of the model in the ERA-Interim might lead to an old bias.

3.3 Vertical profiles of the mean age

A detailed comparison of the vertical profiles of the calculated mean ages with those derived from observations of middle stratosphere balloon flights (Andrews et al., 2001b; Ray et al., 1999) and from SF_6 MIPAS profiles is shown in Fig. 6. According to Stiller et al. (2008), the systematic errors of SF_6 ages are such that ages are 0 to 1 yr too old between 25 and 35 km. In the tropics, the ages from SF_6 MIPAS are higher than those from in situ measurements at all altitudes. The diabatic ages are in good agreement with the in situ measurements up to 28 km and with SF6 ages above 30 km. The seasonal dispersion is much smaller than the discrepancy between in situ and satellite data. The mean diabatic age increases almost uniformly in z from 18 to 34 km at a rate of 0.35 yr km^{-1}.

In the mid-latitudes, there is a good agreement between in situ and satellite observations, except for the SF_6 profiles of Harnisch et al. (1996) above 25 km. The diabatic ages follow the main group of observations, being slightly on the younger side during summer below 20km. The age increases from 16 to 28 km at a rate of 0.4 yr km^{-1} and exhibits only a weak vertical gradient above 28 km, consistently with the findings by Waugh and Hall (2002).

At high latitude during winter, the descent of mesospheric air within the vortex and on its edge induces strong contrast between in vortex and out of vortex air which shows up as the difference between winter and summer profiles below 22 km. Above 25 km there is a small difference between winter and summer as in the mid-latitudes.

The mean diabatic ages agree with SF_6 ages derived from Harnisch et al. (1996) in vortex observations and MIPAS up to 28 km. They depart from other in situ observations by one to two years over the whole altitude range.

Above 28 km, the SF_6 ages from MIPAS exhibit a positive departure which is consistent with the partial photo-chemical dissociation of SF_6 in the mesosphere (Stiller et al., 2012).

The differences between our results and those of Monge-Sanz et al. (2012), mentioned in the previous subsection, are best seen by comparing the vertical profiles in the upper panels of their Fig. 1 to our Fig. 6. In the low and mid-latitudes, at 20 km our ages are similar to those from the calculations of Monge-Sanz et al. (2012) using the ERA-Interim analysis. They are older by one year at 65° N. At higher levels our ages match those from the less diffusive calculation of Monge-Sanz et al. (2012) using ERA-Interim forecasts except at 65° N where our ages are older by about one year. The differences between our calculations and those of Monge-Sanz et al. (2012) are two folds: a) they use a CTM when we are using Lagrangian calculations and b) they use 2000 perpetuals when we use full historical records for all calculations. As already mentioned, pure Lagrangian calculations are not introducing artificial numerical diffusion which tends to limit old ages. We have some reservation about using single year perpetuals as there is a risk of introducing a bias by freezing the QBO oscillation in one of its phases.

The whole comparison suggests, however, that the ERA-Interim tend to produce older ages than observed, especially at high latitudes.

3.4 Age spectrum

As a significant portion of particles remain in the stratosphere with old ages (see Fig. 1), it is important to consider not only the mean age but also the age spectrum. Figure 7 shows that there is a clear distinction between the tropical and the extra-tropical spectra at 20 km. In the tropics, the distribution of ages is mono-disperse and compact, and decays rapidly to zero for ages above 1 yr indicating that very few particles with old ages return to the tropics from mid-latitudes. In the extra-tropics, the peak is at about 0.5 yr, which is small compared to the mean corrected age of about 3.5 yr. The ages exhibit a long flat tail which extends well to large ages. This age distribution of ages corroborates the existence of fast and slow branches of the Brewer circulation (Bonisch et al., 2009, 2011) even if a secondary maximum is not seen. The fast branch is associated with the particles which have travelled directly and rapidly from the tropics to the mid-latitudes through quasi-isentropic motion (Haynes and Shuckburgh, 2000a; Hoor et al., 2005; Shuckburgh et al., 2009), staying at levels below 450 K. The slow branch corresponds to the deep Brewer-Dobson circulation in which the particles enter the tropical pipe and circulate to high altitudes in the stratosphere. A strong seasonal modulation of the fast branch is observed in the Northern Hemisphere with a younger peak during summer than during winter. The modulation is smaller in the Southern Hemisphere. This variation is associated with the seasonal modulation of the subtropical jet and the meridional exchanges which is larger in the Northern Hemisphere than in the Southern Hemisphere (Hoor et al., 2005; Shuckburgh et al., 2009).

At higher altitudes (see Fig. 7), the age distribution in both the tropics and the extra-tropics shifts to older ages. The tail of the tropical distribution gets thicker with increasing altitude but remains much less developed than the extra-tropical tail up to 30 km, in agreement with the relative isolation of the tropical pipe (Neu and Plumb, 1999). The peak of the tropical distribution is 1 to 2 yr younger than the broader main maximum of the extra-tropical distribution. A striking feature is the presence of oscillations in the distributions with an interval of one year between maxima. These oscillations, already mentioned by Reithmeier et al. (2008) and Li et al. (2012), reach a maximum amplitude at the modal age. They propagate towards old ages with the seasonal cycle and it is remarkable that the phase of the oscillation is the same at all altitudes and in both hemispheres. During boreal winters the maximum occurs for integer ages; a positive shift of three months is added for spring and so on for the other seasons. This is consistent with the interpretation of Reithmeier et al. (2008) that the oscillations are entirely due to the modulation of the mass flux entering the stratosphere which is indeed maximum during boreal winter (Seviour et al., 2011). The decay of amplitude with the age, which is almost perfectly exponential in Li et al. (2012) is due to the repeated and multiplicative action of mixing. A detailed comparison of our results with those of Li et al. (2012) is provided in the supplement http://www.atmos-chem-phys.net/12/12133/2012/acp-12-12133-2012-supplement.pdf. We find again an excellent agreement in the patterns of the age spectrum and its seasonal variability with the sole exception that our phase modulation is still in phase with a maximum winter upwelling at high latitude, in agreement with

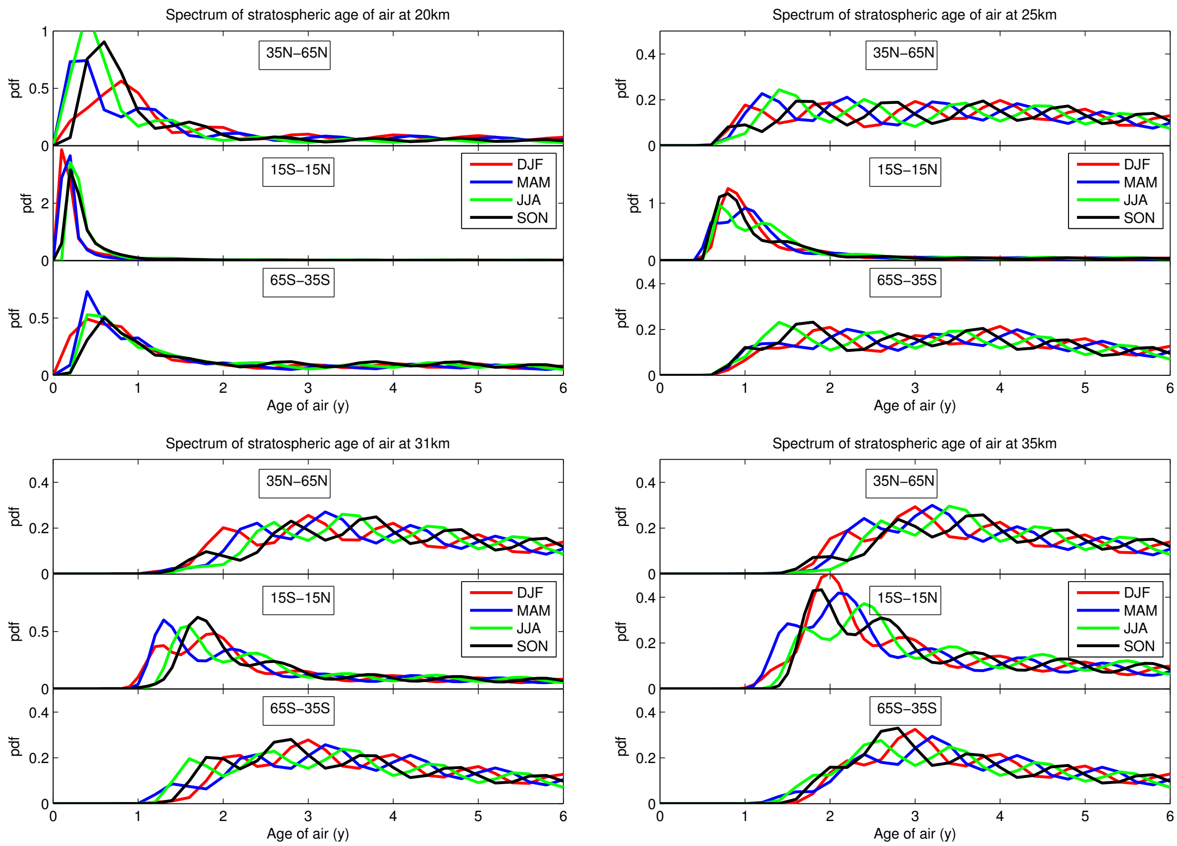

Fig. 7. Age spectra calculated with diabatic trajectories at three altitudes and over three latitude bands. The altitudes are 20 km (upper left), 25 km (upper right), 31 km (lower left) and 35 km (lower right). Each panel shows three latitude ranges: 35° N–65° N (top), 15° S–15° N (mid) and 65° S–35° S (bottom). (Red): winter (DJF) age spectrum averaged over 1989–2010. (Blue): spring (MAM) age spectrum. (Green): summer (JJA) age spectrum. (Black): automn (SON) age spectrum.

Reithmeier et al. (2008), while Li et al. (2012) find that air leaving the tropical region in summer has more chance to reach the polar stratosphere. Finally, it should be stressed that the seasonal modulation of the spectrum does not necessarily show up as a modulation of the mean age when the age distribution is fairly flat as it occurs at 31 and 35 km. This can be checked in Fig. 6 where the profiles are very close in winter, summer and in the annual mean at such levels.

4 Variability and trends

The age of air contains an integrated footprint of the variability of the Brewer-Dobson circulation. The first hint on variability is provided by considering the temporal variation of the number of remaining particles with respect to the mean decay shown in Fig. 1. It is visible (upper left panel of Fig. 8) that the variations are dominated by the annual cycle. The mean annual cycle (lower left panel) exhibits a negative deviation during winter and a positive deviation during summer, implying that more particles cross the tropopause during boreal winter than during summer, consistently with the winter intensification of the tropical upwelling. This annual cycle propagates through ages and it is useful to notice that the amplitude of the cycle is largest for ages of 2 to 3 yr which indicates the duration over which the exiting particles strongly feel the annual cycle. The amplitude decays as age gets older since and remaining particles get uniformly distributed within the stratosphere. This is consistent with the decaying oscillations observed in the age spectra.

The right panel of Fig. 8 shows the percentage of remaining particles after removal of the mean and of the annual cycle. Special events affecting transfers at the tropopause are seen as discontinuities in the vertical whereas variations of the Brewer-Dobson circulation are seen as the oblique patterns.

The most prominent feature is clearly associated with the Pinatubo eruption in June 1991 which induces a reduction of the tropopause crossings and a slowing of the Brewer-Dobson circulation. The impact is strongest on particles with ages of 2 to 3 yr but extends to much older ages and over most of the following decade.

The second smaller pattern after 2008 is possibly due to the cumulative effects of the eruptions of the Soufrières Hills

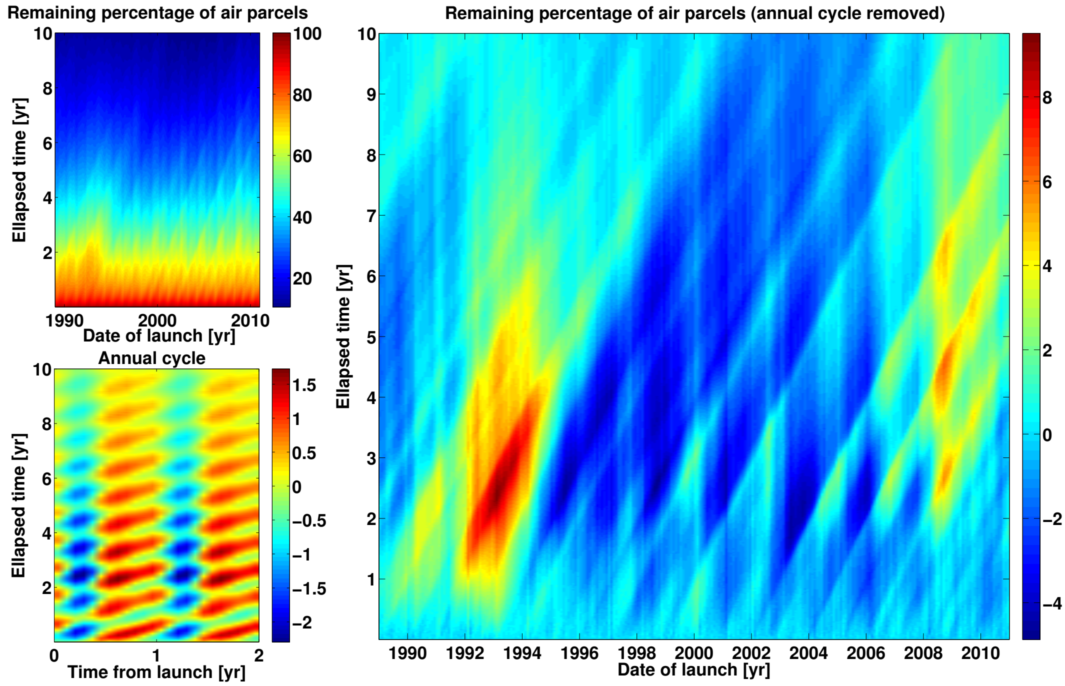

Fig. 8. Upper left: percentage of remaining parcels as a function of time and ellapsed time. Lower left: annual cycle in the percentage shown over two cycles. Right: percentage of remaining parcels after removal of the mean and annual cycle for each ellapsed age.

in May 2006 and Tavurvur in October 2006. As observed by Vernier et al. (2011), the remains of the plumes of these two eruptions have taken about 2 yr to be transported through the depth of the stratosphere (while the Pinatubo plume reached instantly 35 km), which might explain the delay in the stratospheric response.

4.1 Regression method

The temporal evolution of monthly mean diabatic ages at specific altitudes and latitudes (bined as described in Sect. 2.3) has been analysed using a linear response model over the 22 yr of data available from TRACZILLA integrations. This model yields

$$\mathrm{age}(t) = a \cdot t + C(t) + b_1 \cdot \mathrm{qbo}(t - \tau_{\mathrm{qbo}}) + b_2 \cdot \mathrm{enso}(t - \tau_{\mathrm{enso}}) + \epsilon(t) \quad (4)$$

where qbo is a normalised quasi-biennial oscillation index from CDAS/Reanalysis zonally averaged winds at 30 hPa and enso is the normalised Multivariate El Niño Southern Oscillation Index (MEI) (Wolter and Timlin, 1993, 1998), both provided by the NOAA website. The coefficients are a linear trend a, the annual cycle $C(t)$ (12 coefficients), the amplitude b_1 and the delay τ_{qbo} associated to QBO and the amplitude b_2 and the delay τ_{enso} associated to ENSO. The constraint applied to determine the 17 parameters a, b_1, b_2, τ_{qbo}, τ_{enso} and C is to minimise the residual $\epsilon(t)$ in the least square sense. As the combination of amplitude and delay introduces a non linear dependency, there are multiple minima which are sorted out as described in Sect. 4.3.

Here we discard the influence of Pinatubo because there is no simple index suitable to describe the effect of this single event on the Brewer-Dobson circulation and we also neglect solar forcing, because our dataset covers only two solar periods.

4.2 Annual cycle

The annual cycles calculated by the minimising procedure (which takes in account all the factors of variability together) or by a simple monthly composite over the 22 yr turn out to be almost identical.

Figure 9 shows the amplitude of the annual cycle and its phase calculated by fitting a pure annual cosine variation to the full annual cycle. The phase of the cosine is defined to be zero in mid-January. The amplitude is maximum in the extratropical lowermost stratosphere with peak values of about one year at all latitudes in the Northern Hemisphere and of half a year, except at high latitudes, in the Southern Hemisphere. The phase is in opposition between the two hemispheres, the maximum being in mid-March for the Northern Hemisphere and mid-September in the Southern Hemisphere. This maximum signal at the end of the winter is consistent with the reinforced barrier effect of the jet and a stronger descent of old air due to the intensification of the deep Brewer-Dobson circulation during winter (Holton et al., 1995; Waugh and Hall, 2002). In turn, younger ages are observed during summer and autumn. Above 25 km, where the amplitude modulation is less than 0.5 yr, the phase is in

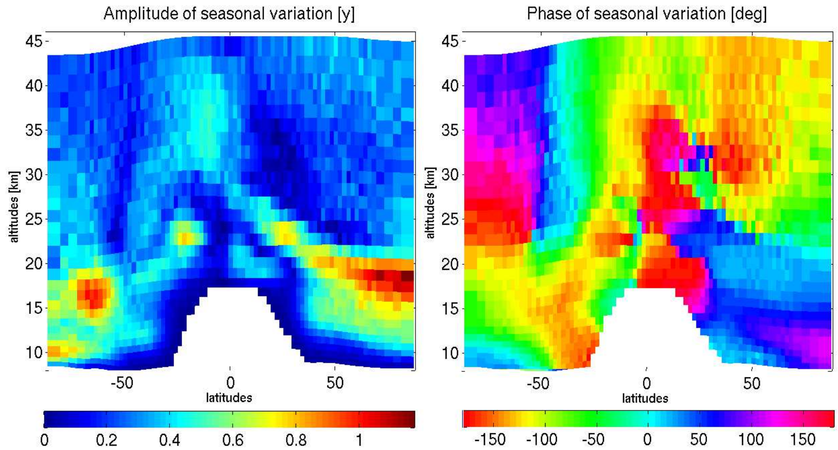

Fig. 9. Altitude-latitude cross-sections of amplitudes (left) and phases (right) of the annual variation derived from least squares method applied on the mean age of air.

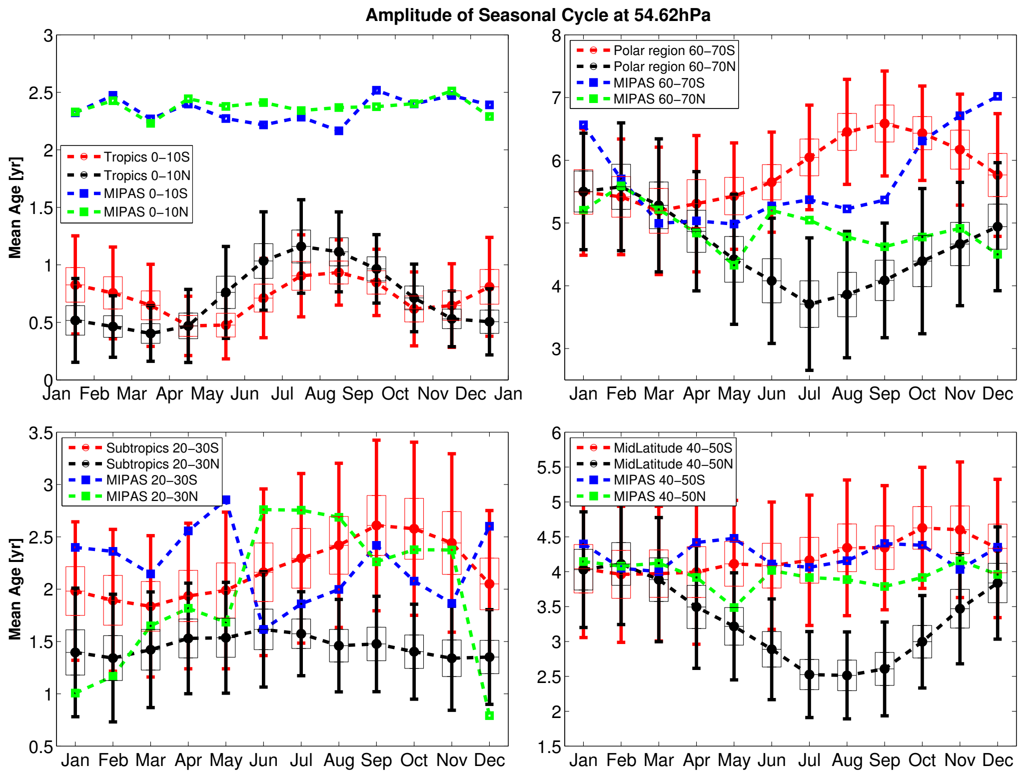

Fig. 10. Amplitude of the seasonal cycle of the mean age over 22 yr at 20 km height in the inner tropics (upper left: 0–10° S and N), in the subtropics (lower left: 20–30° S and N), in the mid-latitudes (lower right: 40–50° N and S) and the polar regions (upper right: 60–70° N and S) compared with the age derived from SF_6 MIPAS data.(Red and blue): Southern Hemisphere for model and SF_6 ages, respectively. (Black and green): same for Northern Hemisphere. The error bars show the standard deviation of the monthly ages and the boxes show the 90% confidence interval of the mean age.

opposition with the extra-tropical lowermost stratosphere. At these altitudes, the stronger descent during winter favours the replacement of old air by younger air detrained from the tropical pipe. The maximum modulation in the Southern Hemisphere is found at 60° S and is associated with the strong descent occurring on the polar vortex edge during late winter and spring (Mariotti et al., 2000).

The enhanced penetration of subtropical and tropical air masses in the extra-tropics during summer and autumn, due to a decreased barrier against quasi-horizontal transport

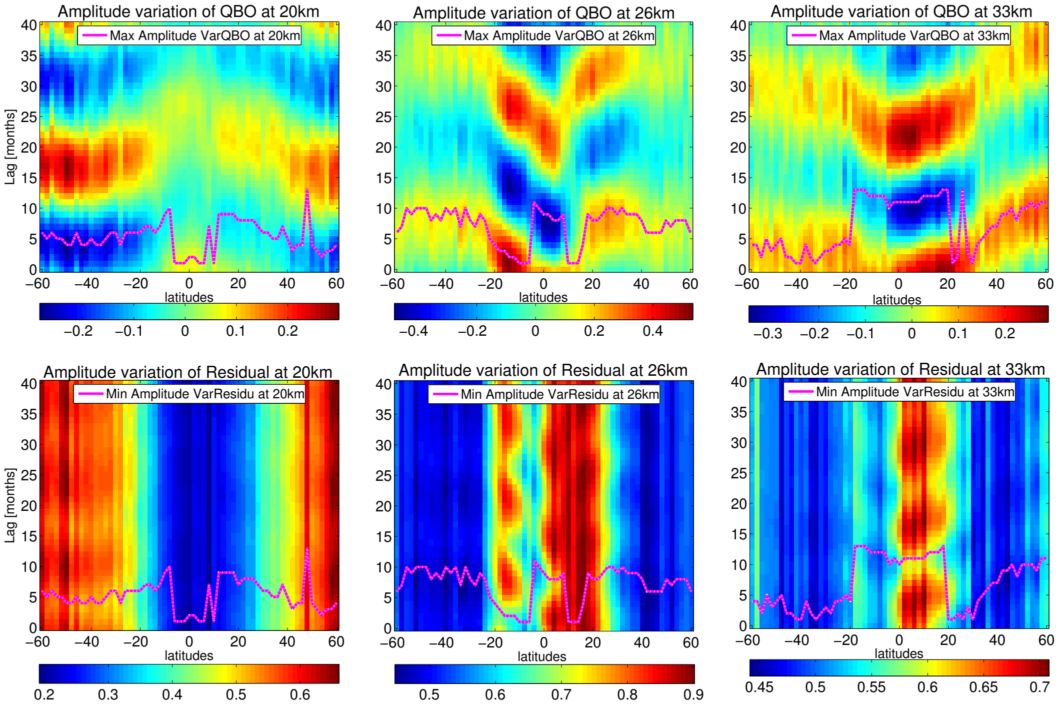

Fig. 11. Time-latitude cross-sections of the amplitude variation of the QBO component (upper) and residual (lower) at altitudes 20 km, 26 km and 33 km as a function of the lag τ_{qbo} with respect to CDAS QBO index. The magenta curves show the lag which maximizes the QBO component in the upper panels and which mimimizes the residual in the lower panels as a function of latitude. Amplitudes are in yr and each panel has its own scale.

and mixing at the subtropical jet, is consistent with previous works on stratosphere-troposphere exchanges, based on tracer's observations (Hoor et al., 2005; Krebsbach et al., 2006; Sawa et al., 2008) or on model simulations (Chen, 1995; Haynes and Shuckburgh, 2000b; Sprenger and Wernli, 2003). It is also consistent with our findings on the age spectrum and those by Bonisch et al. (2009).

In the tropics, the annual modulation above the tropopause and in the tropical pipe rarely exceeds 0.5 yr. In the Northern Hemisphere, it is confined below 30 km with a maximum during summer. In the Southern Hemisphere, it is confined between 30 and 40 km with a maximum at the end of the winter. As already mentioned, the annual modulation is very similar to that described by Li et al. (2012) (see the Supplement).

The seasonal modulation is shown with more details at 55 hPa (about 20 km) in Fig. 10 where the diabatic ages are compared with ages derived from MIPAS SF_6 data (Stiller et al., 2012). It is visible that the Northern Hemisphere modulation is larger in the tropics and in the extra-tropics while the Southern Hemisphere modulation is larger in the subtropics. At high latitudes, both hemispheres exhibit the same amplitude. It is also visible that if SF_6 ages and diabatic ages are of similar amplitude at mid and high latitudes, their seasonal variation are not related.

4.3 Quasi-Biennal-Oscillation and ENSO

Because of the presence of lags in the QBO and ENSO terms in Eq. (4), the problem is non linear and the residual may have multiple minima as a function of the parameters. In order to determine the optimal values of τ_{qbo} and τ_{enso}, the residual is first minimized at fixed lag and then over a range of lags. This is done in sequence for QBO and ENSO. Figure 11 shows the variations of the QBO amplitude coefficient and the residual amplitude as a function of latitude and lag at several levels in the vertical, roughly corresponding to 20, 25 and 30 km height. In most cases, the minimum residual corresponds also to a maximum of the QBO amplitude coefficient in absolute value and the QBO correlates with the age over more than one period. The optimal lag strongly depends on latitude, varying, e.g., by more than a year between 0 and 20° S at 25 km.

Figure 12 shows the amplitudes and lags of the QBO and ENSO contributions to the variability of the age of air. The QBO modulation reaches 0.6 yr with a lag of about 8 months in the tropics near 30 km, with a stronger component in the Northern Hemisphere. This region has already been identified as displaying the largest variability in the age of air in Fig. 2. The influence of the QBO extends upward in the tropical pipe and towards the extratropical stratosphere in both hemispheres with amplitudes of the order of 3 months. The

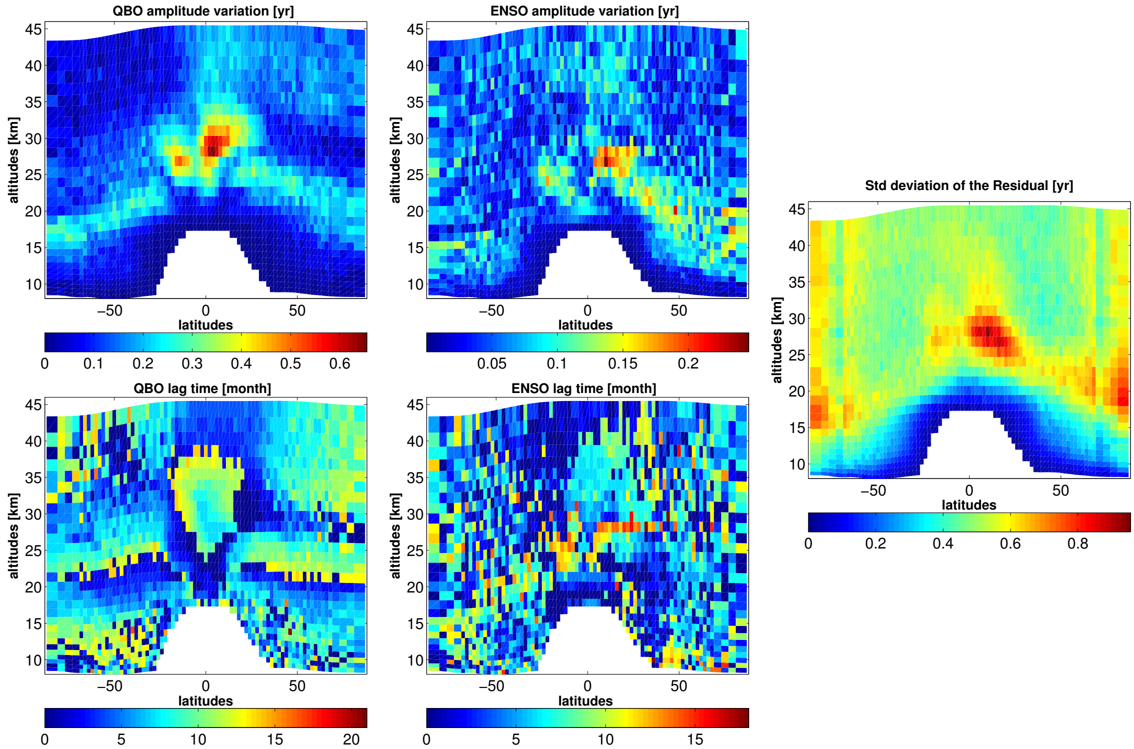

Fig. 12. (Left): altitude-latitude cross-sections of the amplitude of the age variations attributed to the QBO (upper) and its lag with respect to the CDAS QBO index (lower). (Mid): same for the amplitude and lag of the age variability correlated with ENSO MEI index. (Rigth): standard deviation of the residual in Eq. (4).

phase lag with respect to the wind at 30 hPa is fairly symmetric with respect of the equator and varies most rapidly with latitude near 25 km. The dependence on ENSO is much less pronounced (less than 0.2 yr) and bound mostly to the lower stratosphere in the Northern Hemisphere.

The standard deviation of the residual in Eq. (4), shown in the right panel of Fig. 12, is larger than the signal explained by QBO and ENSO and is maximum in the same regions as the QBO. Hence, the variability not linked to QBO and ENSO dominates the age of air at any location in the stratosphere.

4.4 Trends

One should be cautious when estimating a trend in the ERA-Interim, because the reanalysis system cannot be considered time invariant, due to numerous changes in the observations, in particular the introduction of new satellite instruments. Such changes are liable to induce biases in the atmospheric circulation in spite of the attention devoted to avoid them (Dee et al., 2011). It is nevertheless useful to determine the trends, and to compare and eventually reconcile them with observations.

As for the annual cycle, the trends calculated by the minimising procedure (which takes in account all the factors of variability together) or by a simple linear fit turn out to be almost identical. The trend is shown as a function of latitude and altitude in Fig. 13 (left panel). The trend is negative within the lower stratosphere with a larger magnitude in the tropics and the Southern Hemisphere, of the order of $-0.3\,\mathrm{yr\,dec^{-1}}$, than in the Northern Hemisphere. The trend is positive in the extra-tropics above 25 km. In the tropics, the situation is contrasted between the Southern Hemisphere where the trend is negative up to 33 km and the Northern Hemisphere where it is positive above 28 km. The maxima of the trend are located where the amplitude of the QBO modulation is also the largest.

The significance of the trend has been assessed, following von Storch and Zwiers (1999), by performing a Student's t-test among the 264 months of our record using an equivalent number of degrees of freedom calculated as in Zwiers and von Storch (1995) and Bence (1995) (see Appendix). This equivalent number ranges between 35 and 80 in the region of maximum negative trend. The right panel of Fig. 13 shows the one-sided p-value of the Student's test for the hypothesis of a null trend. It is visible that the whole region of large negative trend is highly significant. Although such a simple test is known to overestimate the significance in many cases (Zwiers and von Storch, 1995) and we neglect sub-monthly contribution to the mean age variance, this is an indication that the negative trend in the lower stratosphere is a robust

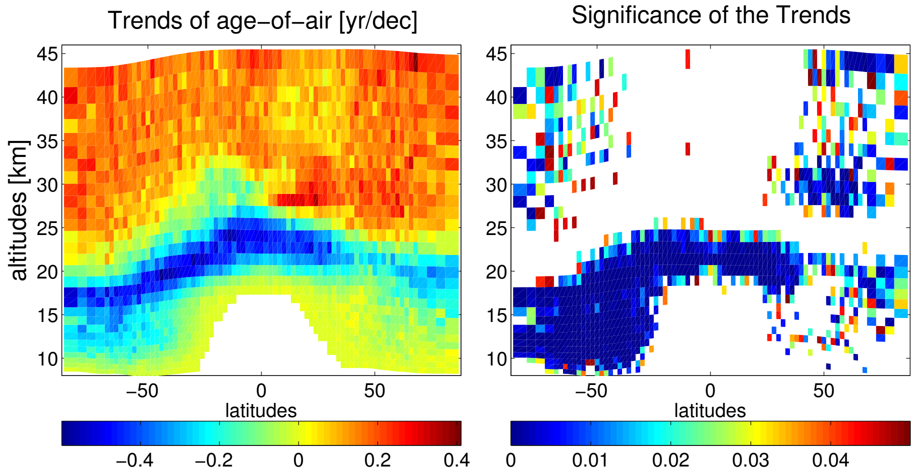

Fig. 13. (Left): altitude-latitude cross-sections of the age trend derived from linear regression over the 22 yr of available data. (Right): p-value of its associated Student statistical test of significance where the p-value is less than 0.05.

feature. On the opposite, we do not find any area of consistent significance above 25 km except perhaps near 60° N and 30 km. In the tropics near 30 km, the p-value is 0.30.

The observed negative trend in the lower stratosphere is consistent with the finding of an acceleration of the shallow branch of the Brewer-Dobson circulation by Bonisch et al. (2011). The positive trend in the mid and high latitudes above 25 km, of the order of 0.2 yr dec^{-1} is consistent with the findings of Engel et al. (2009) and Stiller et al. (2012). It is, however ten times larger than the value found by Monge-Sanz et al. (2012) using the same data. In order to assess better the contributions to the age of air, Fig. 14 shows three illustrative cases. The first case is chosen at 20 km and 60° N, because the amplitude of the annual cycle is the largest and indeed dominates the variability of the age of air, the QBO component being much smaller. The second case is chosen at 28 km and 4° N, because the QBO component dominates the variability over the annual cycle. The ENSO component makes a negligible contribution in both cases. The trend is negative of -0.29 yr dec^{-1} in the first case and slightly positive of 0.11 yr dec^{-1} in the second case. The age fluctuations are large in the second case, so that the trend is hardly significant. In the first case, it is visible that the last section of the record, after 2004, would suggest a positive trend while the negative trend over the whole period has a p-value of 0.02. The third case is chosen at 19.7 km and 40° S, because the trend exhibits its largest value of -0.56 yr dec^{-1}. This is obtained in spite of a flattening or a very slight increase over the last period but it is also visible that the period following the Pinatubo eruption exhibits increased ages which significantly contribute to the trend. The amplitude of this effect is tested by recalculating the trend after removing the period mid-1991 to the end of 1994, leading to a reduced value of -0.33 yr dec^{-1}. It is thus clear that the age of air undergoes decadal scale variability, induced by volcanoes and other less known processes, which may affect trends calculated over durations of a few decades. Our own estimate, based on 22 yr of estimated ages is prone to such effect and our statistical test is not made against such decadal variability.

We compare now our calculations to the age of air obtained by Stiller et al. (2012) using SF_6 data from the MIPAS instrument on board ENVISAT over the period 2002–2010 (see Fig. 15). The comparisons are performed at three altitudes (16.5, 20 and 25 km) and four bands of latitudes (30° S–20° S, 20° S–10° S, 40° N–50° N, 70° N–80° N). There is an old bias of SF_6 ages at 16.5 km at all latitudes and at 20 km in the tropics with respect to our calculations. The tropical bias, which was already noticed on Fig. 5 appears as “robust” in the sense that the dispersion of SF_6 ages is much smaller than the bias. The other panels show a good agreement between our estimations and SF_6 ages. A striking feature is that the age of air tends to flatten or to rise in most locations over the 2002–2010 period, even when a clear negative trend is found over the 22-yr period. This is also in agreement with Stiller et al. (2012) who found a well-spread positive trend over 2002–2010 although there is a disagreement in some locations, for example at 25 km and 70° N–80° N. This is, however, where the statistics are noisy and the trends unreliable.

5 Conclusions

We have performed direct calculations of the stratospheric age of air using Lagrangian trajectories guided by reanalysed winds and heating rates from the ERA-Interim. This study is based on 32 yr of data and provides estimates of the age over the last 22 yr of the dataset (1989–2010). This study complements previous works on the Brewer-Dobson circulation in the ERA-Interim (Iwasaki et al., 2009; Garny et al., 2011;

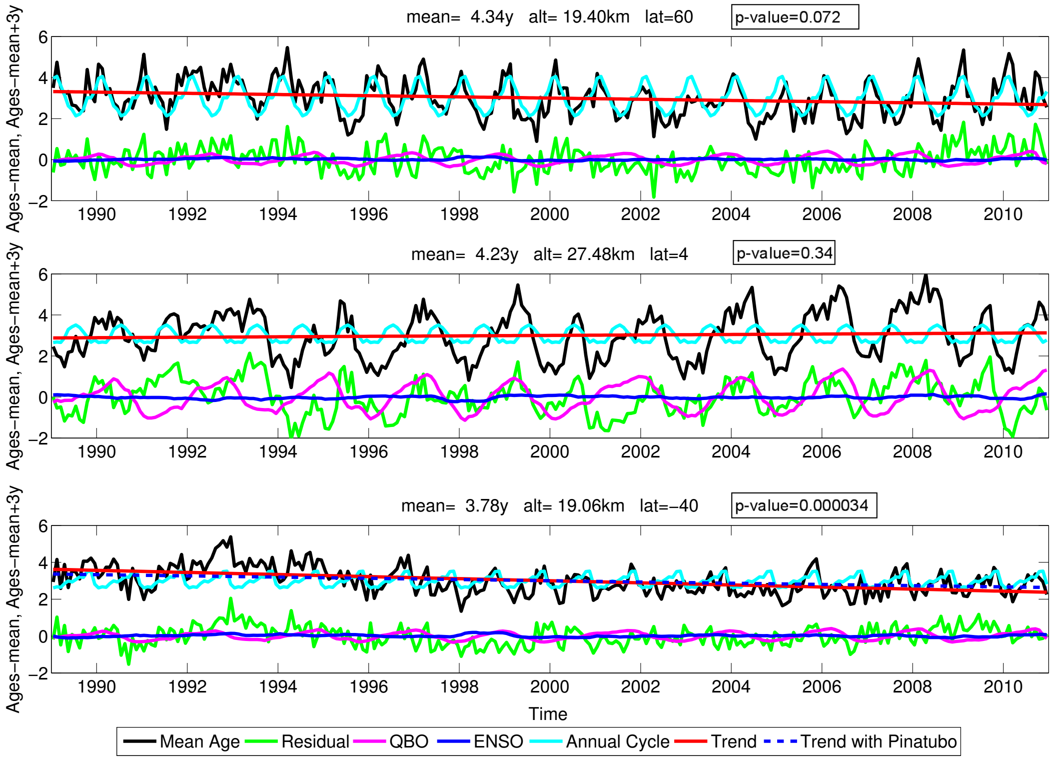

Fig. 14. Temporal evolution of the different components of mean age at several heights and latitudes. (Upper): 20 km and 60° N, (Mid): 28 km and 4° N, (Lower): 20 km and 40° S. (Black): mean age over 22-yr period. (Green): residual of the least squares method. (Magenta): amplitude of the QBO component. (Blue): amplitude of the ENSO component. (Cyan): annual cycle of the mean age. (Red): trend of the mean age derived from the least squares method. (Dash blue): trend of the mean age derived from the least squares method after removal of the Pinatubo years. The *p*-value of the trend is shown in a box for each panel.

Seviour et al., 2011) based on residual velocities which did not take into account stirring and mixing.

Our analysis corroborates the significant improvement of the stratospheric circulation in the ERA-Interim compared to the older ERA-40, as previously noted by other recent works (Monge-Sanz et al., 2007, 2012; Fueglistaler et al., 2009b; Dee et al., 2011; Seviour et al., 2011). In contrast with the ERA-40, diabatic heating rates provide younger ages than the kinematic velocity, a feature shared with the MERRA reanalysis (Schoeberl and Dessler, 2011) but which is not yet properly understood.

On the overall, the agreement between the diabatic ages and observations is very good at low and mid-latitudes but for the SF_6 ages in the tropics. At high latitude, the diabatic ages agree with SF_6 ages but are older than other observations.

The comparison with GEOSCCM (Li et al., 2012) (see Supplement) demonstrates that a state-of-the-art CCM and the ERA-Interim generate very similar patterns of the stratospheric age, in the mean, the annual variations and the age spectrum. The old bias of the ERA-Interim ages with respect to GEOSCCM and other CCMs (Butchart et al., 2010) entirely disappears, without changing the patterns, when parcels reaching above $\theta = 1800\,\mathrm{K}$ are discarded from the calculation. This is puzzling because CCMs have very different upper lids, sometimes above the ERA-Interim (like GEOSCCM) but many times below, and suggests that the old bias of ERA-Interim with respect to the CCMs may arise from a variety of factors.

The age spectrum corroborates that the lower extratropical stratosphere contains young air coming from the mass residual circulation (Birner and Bonisch, 2011) and horizontal mixing, both combined in the lower branch of the Brewer-Dobson circulation. At higher altitude, the age spectrum reveals peaks spaced by annual intervals that propagate on the spectrum with the seasonal cycle and are associated with the annual modulation of the Brewer-Dobson circulation. These modulations do not necessarily show up or weakly when the sole mean age is considered. While the age spectrum is hardly accessible from observations without hypothesis on its shape (Andrews et al., 2001b; Schoeberl et al., 2005; Bonisch et al., 2009), we suggest that it would be useful to expand its usage within the framework of model inter-comparisons as it contains much more informations on the stratospheric circulation than mean age only.

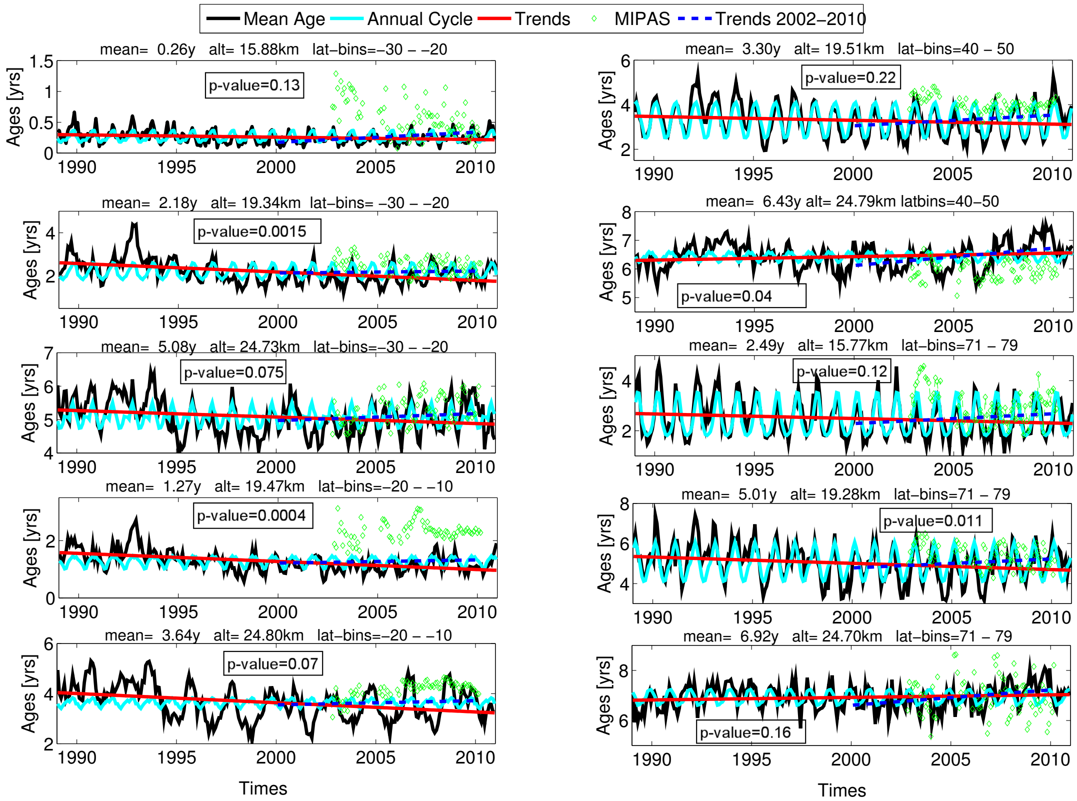

Fig. 15. Evolution of mean age compared with SF_6 ages at several heights and latitudes. (Three first rows of left column): southern subtropics (30° S to 20° S) at 16.5, 20 and 25.5 km. (Last two rows of left column): inner tropics (20° S to 10° S) at 20 and 25.5 km. (Two first rows of right column): northern mid-latitudes (40° N to 50° N) at 17 and 20 km. (Three last rows of right column): northern polar region (71° S to 79° N) at 16.5, 20 and 25.5 km. (Black): mean age. (Cyan): annual cycle of the mean age. (Red): trend of the mean age derived from the least squares method. (Green diamond): SF_6 MIPAS data. (Dash blue): trend of the mean age derived from the least squares method over 2000–2010. The p-value of the trend is shown in a box for each panel.

The variability of mean age as a function of latitude and altitude had been analysed as a linear combination of several contributions: annual cycle, QBO, ENSO and trend. The annual variability dominates in the extra-tropical lower stratosphere below 25 km with higher amplitude, reaching 1.5 yr, in the extra-tropical Northern Hemisphere than in the Southern Hemisphere. The age reaches its maximum during February–March in the Northern Hemisphere and during August–September in the Southern Hemisphere. This is in agreement with a reduction of the shallow branch of the Brewer-Dobson circulation and an intensification of the deep branch during the winter in each hemisphere which has been described in many studies (e.g. Iwasaki et al., 2009; Garcia et al., 2011; Seviour et al., 2011) but it has little relation with the annual modulation as derived by Stiller et al. (2012). In the tropics, the amplitude of the annual modulation does not exceed six months and is basically in opposition with the modulation of the tropical upwelling which reaches its maximum during boreal winter.

The QBO modulation is mostly pronounced within the tropics between 25 and 35 km where its maximum reaches 6 months. The ENSO signal is found to be small and noisy, with a maximum value of about 3 months, and limited to the lower northern stratosphere. This does not contradict the recent finding that warm ENSO events accelerate the upwelling in the lowermost tropical stratosphere (Calvo et al., 2010).

According to these ERA-Interim calculations, a negative trend of the order of -0.2 to $-0.4\,\mathrm{yr\,dec^{-1}}$ is found in the lower stratosphere of the Southern Hemisphere and under 40° N in the Northern Hemisphere below 25 km. A positive trend of 0.2 to $0.3\,\mathrm{yr\,dec^{-1}}$ is found in the mid extra-tropical stratosphere above 25 km. The negative trend is significative with respect to a test that ignores the decadal variations of the stratospheric circulation. It is, however, influenced by the Pinatubo eruption and reduced when the Pinatubo years are removed. The positive trend is marginally significant but is consistent with studies based on in situ and satellite observations (Engel et al., 2009; Stiller et al., 2012). The positive trend in our calculation is increased if only the decade 2000–2010 is considered and this is consistent with the strong positive trend found by Stiller et al. (2012) over the same period.

The whole pattern suggests that the shallow and deep branches of the Brewer-Dobson circulation have not recently evolved in the same direction. The trends are consistent with the recent conclusions of Ray et al. (2010), that the increase in the tropical upwelling documented by Randel et al. (2006) is associated with an acceleration of the shallow branch of the Brewer-Dobson circulation (Bonisch et al., 2011) while the deep branch does not change or slightly weakens. Such pattern is plausible if the shallow and deep branches are controlled by different processes (Gerber, 2012).

CCMs and studies based on residual circulation all predict an increased Brewer-Dobson circulation in the whole stratosphere of 2 to 3 % per decade (McLandress and Shepherd, 2009; Iwasaki et al., 2009; Butchart et al., 2010; Garny et al., 2011; Garcia et al., 2011; Seviour et al., 2011). The discrepancy with our results and those of Engel et al. (2009) and Stiller et al. (2012) might arise from the fact that the age of air does not only depend on the residual circulation but also on the stirring and mixing properties of the stratospheric motion. Owing to their limited resolution, CCMs may not necessarily represent well the mixing properties. A separate diagnostic of the isentropic mixing was performed by Ray et al. (2010) who found a large dispersion between reanalysis but concluded that mixing properties may have varied recently. Such study remains to be done for the ERA-Interim.

It is difficult to estimate a reliable long-term trend from only 22 yr of data. There are evidences that volcanic eruptions, ENSO and other badly represented processes like solar variations may affect the stratospheric circulation over decadal scale. An other factor is ozone depletion to which a significant part of the recent evolution of the Brewer-Dobson circulation has been attributed by Li et al. (2008).

There are also limitations due to the fact that a reanalysis dataset like the ERA-Interim is based on a single model but on a constantly changing observation systems. For instance it is known that the introduction of AMSU-A data in 1998 (Dee and Uppala, 2009) or the introduction of radio-occultation data at the end of 2006 (Poli et al., 2010) had significant impact on the stratospheric temperature. To which extend these changing biases may affect the age of air calculations remains to be determined. It is also worth mentioning that the budget of a reanalysis system, both for heat and momentum, is not closed but is biased by the assimilation increment. Such biases may affect trajectory calculations and residual velocities. It is known, however, that the biases are significantly reduced in the ERA-Interim with respect to previous reanalysis (Fueglistaler et al., 2009b; Dee et al., 2011).

Finally the understanding of stratospheric circulation is limited by the poor accuracy and sparseness of available measurements of the mean age of air from tracers. More observations and in situ measurements combined with new processing of available data (see, e.g. Foucher et al., 2011) will improve our understanding.

Appendix A

Equivalent sample size

The equivalent sample size for a series of the ages $\{a_i\}$, where $i \in [1, N]$, is smaller than N because the ages are correlated. We use the Prats-Winstein formula for the equivalent sample size (Bence, 1995; von Storch and Zwiers, 1999):

$$N_e = N\frac{1-\rho}{1+\rho}, \tag{A1}$$

where

$$\rho = \frac{\sum_{i=1}^{N} a_i a_{i-1}}{\sum_{i=1}^{N-1} a_i^2}.$$

This formula strictly applies to an AR(1) process. By neglecting the periodicities of the age, it provides a conservative lower estimate of the number of degrees of freedom in the series.

The equivalent sample can be used to estimate the standard deviation of the mean as

$$\bar{\sigma} = \sqrt{\frac{1}{N N_e}\sum_{i=1}^{N}(a_i^2 - \bar{a}^2)}$$

where $\bar{a}$ is the mean.

It is also used in the Student test for the mean trend.

Supplementary material related to this article is available online at: http://www.atmos-chem-phys.net/12/12133/2012/acp-12-12133-2012-supplement.pdf.

Acknowledgements. We thank G. Stiller for providing SF_6 age measurements from MIPAS.

Edited by: P. Haynes

cnrs INSU
Institut national des sciences de l'Univers

The publication of this article is financed by CNRS-INSU.

References

Andrews, A. E., Boering, K. A., Daube, B. C., Wofsy, S. C., Hintsa, E. J., Weinstock, E. M., and Bui, T. P.: Empirical age spectra for the lower tropical stratosphere from in situ observations of CO_2: Implications for stratospheric transport, J. Geophys. Res., 104, 26581–26596 doi:10.1029/1999JD900150, 1999.

Andrews, A. E., Boering, K. A., Daube, B. C., Wofsy, S. C., Loewenstein, M., Jost, H., Podolske, J. R., Webster, C. R., Herman, R. L., Scott, D. C., Flesch, G. J., Moyer, E. J., Elkins, J. W., Dutton, G. S., Hurst, D. F., Moore, F. L., Ray, E. A., Romashkin, P. A., and Strahan, S. E.: Mean age of stratospheric air derived from in situ observations of CO_2, CH_4 and N_2O, J. Geophys. Res., 106, 32295–32314, doi:10.1029/2001JD000465, 2001a.

Andrews, A. E., Boering, K. A., Wofsy, S. C., Daube, B. C., Jones, D. B., Alex, S., Loewenstein, M., Podolske, J. R., and Strahan, S. E.: Empirical age spectra for the lower tropical stratosphere from in situ observations of CO_2: quantitative evidence for a sub-tropical barrier to horizontal transport, J. Geophys. Res., 106, 32295–32314, doi:10.1029/2001JD000465, 2001b.

Andrews, D. G., Holton, J. R., and Leovy, C. B.: Middle Atmosphere Dynamics, vol. 40 of International Geophysics Series, Academic Press, San Diego, USA, 1987.

Austin, J. and Li, F.: On the relationship between the strength of the Brewer-Dobson circulation and the age of stratospheric air, Geophys. Res. Lett., 33, L17807, doi:10.1029/2006GL026867, 2006.

Baldwin, M. P., Gray, L. J., Dunkerton, T. J., Hamilton, K., Haynes, P. H., Randel, W. J., Holton, J. R., Alexender, M. J., Hirota, I., Horinouchi, T., Jones, D. B. A., Kinnersley, J. S., Marquardt, C., Sato, K., and Takahashi, M.: The quasi-biennial oscillation, Rev. Geophys., 39, 179–229, doi:10.1029/1999RG000073, 2001.

Bence, J. R.: Analysis of short time series: correcting for autocorrelation, Ecology, 76, 628–639, 1995.

Birner, T. and Bönisch, H.: Residual circulation trajectories and transit times into the extratropical lowermost stratosphere, Atmos. Chem. Phys., 11, 817–827, doi:10.5194/acp-11-817-2011, 2011.

Boering, K. A., Wofsy, S. C., Daube, B. C., Schneider, H. R., Loewenstein, M., Podolske, J. R., and Conway, T. J.: Stratospheric mean ages and transport rates from observations of carbon dioxide and nitrous oxide, Science, 274, 1340–1343, doi:10.1126/science.274.5291.1340, 1996.

Bönisch, H., Engel, A., Curtius, J., Birner, Th., and Hoor, P.: Quantifying transport into the lowermost stratosphere using simultaneous in-situ measurements of SF_6 and CO_2, Atmos. Chem. Phys., 9, 5905–5919, doi:10.5194/acp-9-5905-2009, 2009.

Bönisch, H., Engel, A., Birner, Th., Hoor, P., Tarasick, D. W., and Ray, E. A.: On the structural changes in the Brewer-Dobson circulation after 2000, Atmos. Chem. Phys., 11, 3937–3948, doi:10.5194/acp-11-3937-2011, 2011.

Butchart, N. and Scaife, A. A.: Removal of chlorofluorocarbons by increased mass exchange between the stratosphere and troposphere in a changing climate, Nature, 410, 799–802, doi:10.1038/35071047, 2001.

Butchart, N., Scaife, A. A., Bourqui, M., De Grandpré, J., Hare, S. H. E., Kettleborough, J., Langematz, U., Manzini, E., Sassi, F., Shibata, K., Shindell, D., and Sigmond, M.: Simulation of anthropogenic change in the strength of Brewer-Dobson circulation, Clim. Dynam., 27, 727–741, doi:10.1007/s00382-006-0162-4, 2006.

Butchart, N., Cionni, I., Eyring, V., Shepherd, T. G., Waugh, D. W., Akiyoshi, H., Austin, J., Brühl, C., Chipperfield, M. P., Cordero, E., Dameris, M., Deckert, R., Dhomse, S., Frith, S. M., Garcia, R. R., Gettelman, A., Giorgetta, M. A., Kinnison, D. E., Li, F., Mancini, E., McLandress, C., Pawson, S., Pitari, G., Plummer, D. A., Rozanov, E., Sassi, F., Scinocca, J. F., Shibata, K., Steil, B., and Tian, W.: Chemistry-Climate Model simulations of twenty-first century stratospheric climate and circulation changes, J. Climate, 23, 5349–5374, doi:10.1175/2010JCLI3404.1, 2010.

Calvo, N., Garcia, R. R., Randel, W. J., and Marsh, D. R.: Dynamical mechanism for the increase in tropical upwelling in the lowermost tropical stratosphere during warm ENSO events, J. Atmos. Sci., 67, 2331–2340, doi:10.1175/2010JAS3433.1, 2010.

Chen, P.: Isentropic cross-tropopause mass exchange in the extratropics, J. Geophys. Res., 100, 16661–16674, doi:10.1029/95JD01264, 1995.

Dee, D. and Uppala, S.: Variational bias correction of satellite radiance data in the ERA-Interim reanalysis, Q. J. Roy. Meteorol. Soc., 135, 1830–1841, doi:10.1002/qj.493, 2009.

Dee, D. P., Uppala, S. M., Simmons, A. J., Berrisford, P., Poli, P., Kobayashi, S., Andrae, U., Balmaseda, M. A., Balsamo, G., Bauer, P. Bechtold, P., Beljaars, A. C. M., van de Berg, L., Bidlot, J., Bormann, N., Delsol, C., Dragani, R., Fuentes, M., Geer, A. J., Haimberger, L., Healy, S. B., Hersbach, H., Hólm, E. V., Isaksen, L., Kållberg, P., Köhler, M., Matricardi, M., McNally, A. P., Monge-Sanz, B. M., Morcrette, J.-J., Park, B.-K., Peubey, C., de Rosnay, P., Tavolato, C., Thépaut, J.-N., and Vitart, F.: The ERA-Interim reanalysis: configuration and performance of the data assimilation system, Q. J. Roy. Meteor. Soc., 137, 553–597, doi:10.1002/qj.828, 2011.

Elkins, J. W., Gilligan, J. M., Dutton, G. S., Baring, T. J., Volk, C. M., Dunn, R. E., Myers, R. C., Montzka, S. A., Wamsley, P. R., Hayden, A., H., Butler, J. H., Thompson, T. M., Swanson, T. H., Dlugokencky, E. J., Novelli, P. C., Hurst, D. F., Lobert, J. M., Ciciora, S. J., McLaughlin, R. J., Thompson, T. L., Winkler, R. H., Fasser, P. J., Steele, L. P., and Lucarelli, M. P.: Air-borne gas chromatograph for in-situ measurements of long-lived species in upper troposphere and lower stratosphere, Geophys. Res. Lett., 23, 347–350, doi:10.1029/96GL00244, 1996.

Eluszkiewicz, J., Hemler, R. S., Mahlman, J. D., Bruhwiler, L., and Takacs, L. L.: Sensitivity of age-of-air calculations to the choice of advection scheme, J. Atmos. Sci., 57, 3185–3201, doi:10.1175/1520-0469(2000)057<3185:SOAOAC>2.0.CO;2, 2000.

Engel, A., Möbius, T., Bönisch, H., Schmidt, U., Heinz, R., Levin, I., Atlas, E., Aoki, S., Nakazawa, T., Sugawara, S., Moore, F., Hurst, D., Elkins, J., Schauffler, S., Andrews, A., and Boering, K.: Age of stratospheric air unchanged within uncertainties over the past 30 years, Nature Geosci., 2, 28–31, doi:10.1038/ngeo388, 2009.

Eyring, V., Butchart, N., Waugh, D. W., Akiyoshi, H., Austin, J., Bekki, S., Bodeker, G. E., Boville, B. A., Brühl, C., Chipperfield, M. P., Cordero, E., Dameris, M., Deushi, M., Fioletov, V. E., Frith, S. M., Garcia, R. R., Gettelman, A., Giorgetta, M. A., Grewe, V., Jourdain, L., Kinnison, D. E., Mancini, E., Manzini, E., Marchand, M., Marsh, D. R., Nagashima, T., Newman, P. A., Nielsen, J. E., Pawson, S., Pitari, G., Plummer, D. A., Rozanov, E., Schraner, M., Shepherd, T. G., Shibata, K., Stolarski, R. S., Struthers, H., Tian, W., and Yoshiki, M.: Assessment of temperature, trace species, and ozone in chemistry-climate model simulations of the recent past, J. Geophys. Res., 111, D22308, doi:10.1029/2006JD007327, 2006.

Foucher, P. Y., Chédin, A., Dufour, G., Capelle, V., Boone, C. D., and Bernath, P.: Technical Note: Feasibility of CO_2 profile retrieval from limb viewing solar occultation made by the ACE-FTS instrument, Atmos. Chem. Phys., 9, 2873–2890, doi:10.5194/acp-9-2873-2009, 2009.

Foucher, P. Y., Chédin, A., Armante, R., Boone, C., Crevoisier, C., and Bernath, P.: Carbon dioxide atmospheric vertical profiles retrieved from space observation using ACE-FTS solar occultation instrument, Atmos. Chem. Phys., 11, 2455–2470, doi:10.5194/acp-11-2455-2011, 2011.

Fueglistaler, S., Dessler, A. E., Dunkerton, T. J., Folkins, I., Fu, Q., and Mote, P. W.: Tropical tropopause layer, Rev. Geophys., 47, RG1004, doi:10.1029/2008RG000267, 2009a.

Fueglistaler, S., Legras, B., Beljaars, A., Morcrette, J.-J., Simmons, A., Tompkins, A. M., and Uppala, S.: The diabatic heat budget of the upper troposphere and lower/mid stratosphere in ECMWF reanalyses, Q. J. Roy. Meteor. Soc., 135, 21–37, doi:10.1002/qj.361, 2009b.

Garcia, R. R. and Randel, W. J.: Acceleration of Brewer-Dobson circulation due to the increases in greenhourse gases, J. Atmos. Sci., 65, 2731–2739, doi:10.1175/2008JAS2712.1, 2008.

Garcia, R. R., Randel, W. J., and Kinnison, D. E.: On the determination of age of air trends from atmospheric trace species, J. Atmos. Sci., 68, 139–154, doi:10.1175/2010JAS3527.1, 2011.

Garny, H., Dameris, M., Randel, W., Bodeker, G. E., and Deckert, R.: Dynamically forced increase of tropical upwelling in the lower stratosphere, J. Atmos. Sci., 68, 1214–1233, doi:10.1175/2011JAS3701.1, 2011.

Gerber, E. P.: Stratospheric versus tropospheric control of the strength et structure of the Brewer-Dobson circulation, J. Atmos. Sci., 69, 2857–2877, doi:10.1175/JAS-D-11-0341.1, 2012.

Hall, T. and Plumb, R. A.: Age as a diagnostic of stratospheric transport, J. Geophys. Res., 99, 1059–1070, doi:10.1029/93JD03192, 1994.

Harnisch, J., Borchers, R., Fabian, P., and Maiss, M.: Tropospheric trends for CF_4 and C_2F_6 since 1982 derived from SF_6 dated stratospheric air, Geophys. Res. Lett., 23, 1099–1102, doi:10.1029/96GL01198, 1996.

Haynes, P. H. and Shuckburgh, E.: Effective diffusivity as a diagnostic of atmospheric transport 1. Stratosphere, J. Geophys. Res., 105, 22777–22794, doi:10.1029/2000JD900093, 2000a.

Haynes, P. H. and Shuckburgh, E.: Effective diffusivity as a diagnostic of atmospheric transport 2. Troposphere and lower stratosphere, J. Geophys. Res., 105, 22795–22810, doi:10.1029/2000JD900092, 2000b.

Holton, J. R., Haynes, P. H., McIntyre, M. E., Douglass, A. R., Rood, R. B., and Pfister, L.: Stratosphere-troposphere exchange, Rev. Geophys., 33, 403–440, doi:10.1029/95RG02097, 1995.

Hoor, P., Gurk, C., Brunner, D., Hegglin, M. I., Wernli, H., and Fischer, H.: Seasonality and extent of extratropical TST derived from in-situ CO measurements during SPURT, Atmos. Chem. Phys., 4, 1427–1442, doi:10.5194/acp-4-1427-2004, 2004.

Hoor, P., Fischer, H., and Lelieveld, J.: Tropical and extratropical tropospheric air in the lowermost stratosphere over Europe: a CO-based budget, Geophys. Res. Lett., 32, L13812, doi:10.1029/2005GL022495, 2005.

Iwasaki, T., Hamada, H., and Miyazaki, K.: Comparisons of Brewer-Dobson circulations diagnosed from reanalyses, J. Meteorol. Soc. Jpn., 87, 997–1006, doi:10.2151/jmsj.87.997, 2009.

Kida, H.: General circulation of air parcels and transport characteristics derived from a hemispheric GCM, Part 2, Very long-term motions of air parcels in the troposphere and stratosphere, J. Meteorol. Soc. Jpn., 61, 510–522, 1983.

Krebsbach, M., Schiller, C., Brunner, D., Günther, G., Hegglin, M. I., Mottaghy, D., Riese, M., Spelten, N., and Wernli, H.: Seasonal cycles and variability of O_3 and H_2O in the UT/LMS during SPURT, Atmos. Chem. Phys., 6, 109–125, doi:10.5194/acp-6-109-2006, 2006.

Legras, B., Pisso, I., Berthet, G., and Lefèvre, F.: Variability of the Lagrangian turbulent diffusion in the lower stratosphere, Atmos. Chem. Phys., 5, 1605–1622, doi:10.5194/acp-5-1605-2005, 2005.

Li, F., Austin, J., and Wilson, J.: The strength of the Brewer Dobson circulation in a changing climate: coupled chemistry climate model simulations, J. Climate, 21, 40, doi:10.1175/2007JCLI1663.1, 2008.

Li, F., Waugh, D. W., Douglass, A. R., Newman, P. A., Pawson, S., Stolarski, R. S., Strahan, S. E., and Nielsen, J. E.: Seasonal variations of stratospheric age spectra in the Goddard Earth Observing System Chemistry Climate Model (GEOSCCM), J. Geophys. Res., 117, D05 134, doi:10.1029/2011JD016877, 2012.

Li, S. and Waugh, D. W.: Sensitivity of mean age and long-lived tracers to transport parameters in a two-dimensional model, J. Geophys. Res., 104, 30559–30569, doi:10.1029/1999JD900913, 1999.

Liu, S., Fueglistaler, S., and Haynes, P. H.: The advection-condensation paradigm for stratospheric water vapour, J. Geophys. Res., 115, D24307, doi:10.1029/2010JD014352, 2010.

Mariotti, A., Mechoso, C., Legras, B., and Chi, Y.: The evolution of the ozone "collar" in the Antarctic lower stratosphere during early August 1994, J. Atmos. Sci., 57, 402–414, doi:10.1175/1520-0469(2000)057<0402:TEOTOC>2.0.CO;2, 2000.

McLandress, C. and Shepherd, T. G.: Simulated anthropogenic changes in the Brewer-Dobson circulation, including its extension to high latitudes, J. Climate, 22, 1516, doi:10.1175/2008JCLI2679.1, 2009.

Meijer, E. W., Bregman, B., Segers, A., and van Velthoven, P. F. J.: The influence of data assimilation on the age of air calculated with a global chemistry-transport model using ECMWF wind fields, Geophys. Res. Lett., 31, L23114, doi:10.1029/2004GL021158, 2004.

Monge-Sanz, B. M., Chipperfield, M. P., Simmons, A. J., and Uppala, S. M.: Mean age of air and transport in a CTM: comparison of different ECMWF analyses, Geophys. Res. Lett., 340, L04801, doi:10.1029/2006GL028515, 2007.

Monge-Sanz, B. M., Chipperfield, M. P., Dee, D. P., Simmons, A. J., and Uppala, S. M.: Improvements in the stratospheric transport achieved by a chemistry transport model with ECMWF (re)analyses: identifying effects and remaining challenges, Q. J. R. Meteorol. Soc., doi:10.1002/qj.1996, 2012.

Neu, J. L. and Plumb, R. A.: Age of air in a "leaky pipe" model of stratospheric transport, J. Geophys. Res., 104, 19243–19255, doi:10.1029/1999JD900251, 1999.

Niwano, M., Yamazaki, K., and Shiotani, M.: Seasonal and QBO variations of ascent rate in the tropical lower stratosphere as inferred from UARS HALOE trace gas data, J. Geophys. Res., 108, 4794, doi:10.1029/2003JD003871, 2003.

Pisso, I. and Legras, B.: Turbulent vertical diffusivity in the sub-tropical stratosphere, Atmos. Chem. Phys., 8, 697–707, doi:10.5194/acp-8-697-2008, 2008.

Ploeger, F., Konopka, P., Günther, G., Grooß, J.-U., and Müller, R.: Impact of the vertical velocity scheme on modeling transport in the tropical tropopause layer, J. Geophys. Res., 115, D03301, doi:10.1029/2009JD012023, 2010.

Poli, P., Healy, S. B., and Dee, D. P.: Assimilation of global positioning system radio occultation data in the ECMWF ERA-Interim reanalysis, Q. J. Roy. Meteor. Soc., 136, 1972–1990, doi:10.1002/qj.722, 2010.

Punge, H. J., Konopka, P., Giorgetta, M. A., and Müller, R.: Effect of the quasi-biennial oscillation on low-latitude transport in the stratosphere derived from trajectory calculations, J. Geophys. Res., 114, D03102, doi:10.1029/2008JD010518, 2009.

Randel, W. J., Wu, F., Vömel, H., Nedoluha, G. E., and Forster, P.: Decreases in stratospheric water vapor after 2001: links to changes in the tropical tropopause and the Brewer-Dobson circulation, J. Geophys. Res., 111, D12312, doi:10.1029/2005JD006744, 2006.

Ray, E. A., Moore, F. L., Elkins, J. W., Dutton, G. S., Fahey, D. W., Vomel, H., Oltmans, S. J., and Rosenlof, K. H.: Transport into the Northern Hemisphere lowermost stratosphere revealed by in-situ tracer measurements, J. Geophys. Res., 104, D21304, doi:10.1029/1999JD900323, 1999.

Ray, E. A., Moore, F. L., Rosenlof, K. H., Davis, S. M., Boenisch, H., Morgenstern, O., Smale, D., Rozanov, E., Hegglin, M., Pitari, G., Mancini, E., Braesicke, P., Butchart, N., Hardiman, S., Li, F., Shibata, K., and Plummer, D. A.: Evidence for changes in stratospheric transport and mixing over the past three decades based on multiple data sets and tropical leaky pipe analysis, J. Geophys. Res., 115, D21304, doi:10.1029/2010JD014206, 2010.

Reithmeier, C., Sausen, R., and Grewe, V.: Investigating lower stratospheric model transport: Lagrangian calculations of mean age and age spectra in the GCM ECHAM4, Climate Dynamics, 30, 225–238, doi:10.1007/s00382-007-0294-1, 2008.

Salby, M. L. and Callaghan, P. F.: Interaction between the Brewer Dobson circulation and the Hadley circulation, J. Climate, 18, 4303–4316, doi:10.1175/JCLI3509.1, 2005.

Salby, M. L. and Callaghan, P. F.: Influence of the Brewer-Dobson circulation on stratosphere-troposphere exchange, J. Geophys. Res., 111, D21106, doi:10.1029/2006JD007051, 2006.

Sawa, Y., Machida, T., and H., M.: Seasonal variations of CO_2 near the tropopause observation by commercial aircraft, J. Geophys. Res., 113, D23301, doi:10.1029/2008JD010568, 2008.

Scheele, M. P., Siegmund, P. C., and Velthoven, P. F. J.: Stratospheric age of air computed with trajectories based on various 3D-Var and 4D-Var data sets, Atmos. Chem. Phys., 5, 1–7, doi:10.5194/acp-5-1-2005, 2005.

Schoeberl, M. R. and Dessler, A. E.: Dehydration of the stratosphere, Atmos. Chem. Phys., 11, 8433–8446, doi:10.5194/acp-11-8433-2011, 2011.

Schoeberl, M. R., Douglass, A. R., Zhu, Z., and Pawson, S.: A comparison of the lower stratospheric age spectra derived from a general circulation model and two data assimilation systems, J. Geophys. Res., 108, 4113, doi:10.1029/2002JD002652, 2003.

Schoeberl, M. R., Douglass, A. R., Polansky, B., Boone, C., Walker, K. A., and Bernath, P.: Estimation of stratospheric age spectrum from chemical tracers, J. Geophys. Res., 110, D21303, doi:10.1029/2005JD006125, 2005.

Seviour, W. J. M., Butchart, N., and Hardiman, S. C.: The Brewer-Dobson circulation inferred from ERA-Interim, Q. J. Roy. Meteor. Soc., 138, 878–888, doi:10.1002/qj.966, 2011.

Shu, J., Tian, W., Austin, J., Chipperfield, M. P., Xie, F., and Wang, W.: Effects of sea surface temperature and greenhouse gas changes on the transport between the stratosphere and troposphere, J. Geophys. Res., 116, 0148–0227, doi:10.1029/2010JD014520, 2011.

Shuckburgh, E., D'Ovidio, F., and Legras, B.: Local mixing events in the upper troposphere and lower stratosphere. Part II: Seasonal and interannual variability, J. Atmos. Sci., 66, 3695–3706, doi:10.1175/2009JAS2983.1, 2009.

Sigmond, M. P., Siegmund, P. C., Manzini, E., and Kelder, H.: A simulation of the separate climat effects of middle atmospheric and tropospheric CO_2 doubling, J. Climate, 17, 2352–2367, doi:10.1175/1520-0442(2004)017<2352:ASOTSC>2.0.CO;2, 2004.

Sprenger, M. and Wernli, H.: A northern hemispheric climatology of cross-tropopause exchange for the ERA15 time period (1979–1993), J. Geophys. Res., 108, 8521, doi:10.1029/2002JD002636, 2003.

Stiller, G. P., von Clarmann, T., Hörfner, M., Glatthor, N., Grabowski, U., Kellmann, S., Kleinert, A., Linden, A., Milz, M., Reddmann, T., Steck, T., Fischer, H., Funke, B., López-Puertas, M., and Engel, A.: Global distribution of mean age of stratospheric air from MIPAS SF6 measurements, Atmos. Chem. Phys., 8, 677–695, doi:10.5194/acp-8-677-2008, 2008.

Stiller, G. P., von Clarmann, T., Haenel, F., Funke, B., Glatthor, N., Grabowski, U., Kellmann, S., Kiefer, M., Linden, A., Lossow, S., and López-Puertas, M.: Observed temporal evolution of global mean age of stratospheric air for the 2002 to 2010 period, Atmos. Chem. Phys., 12, 3311–3331, doi:10.5194/acp-12-3311-2012, 2012.

Stohl, A., Forster, C., Frank, A., Seibert, P., and Wotawa, G.: Technical note: The Lagrangian particle dispersion model FLEXPART version 6.2, Atmos. Chem. Phys., 5, 2461–2474, doi:10.5194/acp-5-2461-2005, 2005.

Thompson, D. W. J. and Solomon, S.: Recent stratospheric climat trends as evidence inradiosonde data: Global structure and tropospheric linkages., J. Climate, 18, 4785–4795, doi:10.1175/JCLI3585.1, 2005.

Thompson, D. W. J. and Solomon, S.: Understanding recent stratospheric climate change, J. Climate, 22, 1934–1943, doi:10.1175/2008JCLI2482.1, 2009.

Uppala, S., Kallberg, P., Simmons, A., Andrae, U., da Costa Bechtold, V., Fiorino, M., Gibson, J., Haseler, J., Hernandez, A., Kelly, G., Li, X., Onogi, K., Saarinen, S., Sokka, N., Allan, R., Andersson, E., Arpe, K., Balmaseda, M., Beljaars, A., van de Berg, L., Bidlot, J., Bormann, N., Caires, S., Chevallier, F., Dethof, A., Dragosavac, M., Fisher, M., Fuentes, M., Hagemann, S., Holm, E., Hoskins, B., Isaksen, L., Janssen, P., Jenne, R., McNally, A., Mahfouf, J.-F., Morcrette, J.-J., Rayner, N., Saunders, R., Simon, P., Sterl, A., Trenberth, K., Untch, A., Vasiljevic, D., Viterbo, P., and Woollen, J.: The ERA-40 re-analysis, Q. J. Roy. Meteor. Soc., 131, 2961–3012, doi:10.1256/qj.04.176, 2005.

Vernier, J. P., Thomason, L. W., Pommereau, J. P., Bourassa, A., Pelon, J., Garnier, A., Hauchecorne, A., Trepte, C., Degenstein, D., and Vargas, F.: Major influence of tropical volcanic eruptions on the stratospheric aerosol layer during the last decade, Geophys. Res. Lett., 38, L12807, doi:10.1029/2011GL047563, 2011.

von Storch, H. and Zwiers, F. W.: Statistical Analysis in Climate Research, Cambridge Unv. Press, 1999.

Waugh, D.: Atmospheric dynamics: the age of stratospheric air, Nature Geosci., 2, 14–16, doi:10.1038/ngeo397, 2009.

Waugh, D. and Hall, T.: Age of stratospheric air: theory, observations, and models, Rev. Geophys., 40, 1010, doi:10.1029/2000RG000101, 2002.

Wolter, K. and Timlin, M. S.: Monitoring ENSO in COADS with a seasonally adjusted principal component index, in: Proc. of the 17th Climate Diagnostics Workshop, Oklahoma Clim. Survey, NOAA/NMC/CAC, NSSL, CIMMS and the School of Meteor., Univ. of Oklahoma, Norman, OK, 52–57, 1993.

Wolter, K. and Timlin, M. S.: Measuring the strength of ENSO – how does 1997/98 rank?, Weather, 53, 315–324, 1998.

Zwiers, F. W. and von Storch, H.: Taking serial correlation into account in test of the mean, J. Climate, 8, 336–351, doi:10.1175/1520-0442(1995)008<0336:TSCIAI>2.0.CO;2, 1995.